We recently reported that inhibition of CX3CL1 ameliorated collagen-induced arthritis in mice, probably by suppression of inflammatory cell migration into the synovium (30). Others reported that anti-CX3CR1 Ab treatment blocked inflammatory cell infiltration in the glomeruli, prevented crescent formation, and improved renal function in the Wistar-Kyoto crescentic glomerulonephritis model (49). Furthermore, the gene deletion of CX3CR1 resulted in an ~50% decrease in the formation of atherosclerotic lesions and the number of infiltrated macrophages in the lesion in experimental atherosclerosis mice (50, 51). These results together with our findings suggest that blockade of CX3CL1-CX3CR1 interaction might be therapeutically useful for several diseases associated with inflammatory cell infiltration. In this study we propose that such treatment is also suitable for IIM. To our knowledge, this is the first report demonstrating that a chemokine inhibitor could reduce the severity of myositis.

In conclusion, we demonstrated in the present study that inhibition of CX3CL1 significantly improved histopathological changes in the muscles of EAM mice, suggesting that blockade of CX3CL1 might be therapeutically beneficial for IIM.

Acknowledgments

We thank Dr. Hiroshi Nemoto (Toho University School of Medicine) for providing critical suggestions for the development of EAM mice. We also thank Miyuki Nishimura, Keiko Mizuno, and Yoko Inoue for their excellent technical support.

Disclosures

The authors have no financial conflict of interest.

References

1. Arahata, K., and A. G. Engel. 1984. Monoclonal antibody analysis of mononuclear cells in myopathies. I. Quantitation of subsets according to diagnosis and sites of accumulation and demonstration and counts of muscle fibers invaded by T cells. *Ann. Neurol.* 16: 193–208.
2. Engel, A. G., and K. Arahata. 1984. Monoclonal antibody analysis of mononuclear cells in myopathies. II. Phenotypes of autoinvasive cells in polymyositis and inclusion body myositis. *Ann. Neurol.* 16: 209–215.
3. Dalakas, M. C. 1991. Polymyositis, dermatomyositis and inclusion-body myositis. *N. Engl. J. Med.* 325: 1487–1498.
4. Cherin, P., S. Herson, M. C. Crevon, J. J. Hauw, P. Cervera, P. Galanaud, and D. Emilie. 1996. Mechanisms of lysis by activated cytotoxic cells expressing perforin and granzyme-B genes and the protein TIA-1 in muscle biopsies of myositis. *J. Rheumatol.* 23: 1135–1142.
5. Goebels, N., D. Michaelis, M. Engelhardt, S. Huber, A. Bender, D. Pongratz, M. A. Johnson, H. Wekerle, J. Tschopp, D. Jenne, et al. 1996. Differential expression of perforin in muscle-infiltrating T cells in polymyositis and dermatomyositis. *J. Clin. Invest.* 97: 2905–2910.
6. Tews, D. S., and H. H. Goebel. 1996. Cytokine expression profile in idiopathic inflammatory myopathies. *J. Neuropathol. Exp. Neurol.* 55: 342–347.
7. Lepidi, H., V. Frances, D. Figarella-Branger, C. Bartoli, A. Machado-Bacta, and J. F. Pellissier. 1998. Local expression of cytokines in idiopathic inflammatory myopathies. *Neuropathol. Appl. Neurobiol.* 24: 73–79.
8. Sugiura, T., Y. Kawaguchi, M. Harigai, K. Takagi, S. Ohta, C. Fukasawa, M. Hara, and N. Kamatani. 2000. Increased CD40 expression on muscle cells of polymyositis and dermatomyositis: role of CD40-CD40 ligand interaction in IL-6, IL-8, IL-15, and monocyte chemoattractant protein-1 production. *J. Immunol.* 164: 6593–6600.
9. Lundberg, I. E. 2000. The role of cytokines, chemokines, and adhesion molecules in the pathogenesis of idiopathic inflammatory myopathies. *Curr. Rheumatol. Rep.* 2: 216–224.
10. De Bleecker, J. L., B. De Paepe, I. E. Vanwalleghem, and J. M. Schroder. 2002. Differential expression of chemokines in inflammatory myopathies. *Neurology* 58: 1779–1785.
11. Liprandi, A., C. Bartoli, D. Figarella-Branger, J. F. Pellissier, and H. Lepidi. 1999. Local expression of monocyte chemoattractant protein-1 (MCP-1) in idiopathic inflammatory myopathies. *Acta Neuropathol.* 97: 642–648.
12. Confalonieri, P., P. Bernasconi, P. Megna, S. Galbiati, F. Cornelio, R. Mantegazza. 2000. Increased expression of β-chemokines in muscle of patients with inflammatory myopathies. *J. Neuropathol. Exp. Neurol.* 59: 164–169.
13. Bartoli, C., M. Civatte, J. F. Pellissier, and D. Figarella-Branger. 2001. CCR2A and CCR2B, the two isoforms of the monocyte chemoattractant protein-1 receptor are up-regulated and expressed by different cell subsets in idiopathic inflammatory myopathies. *Acta Neuropathol. (Berl.)* 102: 385–392.
14. De Rossi, M., P. Bernasconi, F. Baggi, R. de Waal Malefyt, and R. Mantegazza. 2000. Cytokines and chemokines are both expressed by human myoblasts: possible relevance for the immune pathogenesis of muscle inflammation. *Int. Immunol.* 12: 1329–1335.
15. Zlotnik, A., and O. Yoshie. 2000. Chemokines: a new classification system and their role in immunity. *Immunity* 12: 121–127.
16. Yoshie, O., T. Imai, and H. Nomiyama. 2001. Chemokines in immunity. *Adv. Immunol.* 78: 57–110.
17. Bazan, J. F., K. B. Bacon, G. Hardiman, W. Wang, K. Soo, D. Rossi, D. R. Greaves, A. Zlotnik, and T. J. Schall. 1997. A new class of membrane-bound chemokine with a CX3C motif. *Nature* 385: 640–644.
18. Pan, Y., C. Lloyd, H. Zhou, S. Dolich, J. Deeds, J. A. Gonzalo, J. Vath, M. Gosselin, J. Ma, B. Dussault, et al. 1997. Neurotactin, a membrane-anchored chemokine upregulated in brain inflammation. *Nature* 387: 611–617.
19. Fraticelli, P., M. Sironi, G. Bianchi, D. D'Ambrosio, C. Albanesi, A. Stoppacciaro, M. Chieppa, P. Allavena, L. Ruco, G. Girolomoni, et al. 2001. Fractalkine (CX3CL1) as an amplification circuit of polarized Th1 responses. *J. Clin. Invest.* 107: 1173–1181.
20. Imaizumi, T., H. Yoshida, and K. Satoh. 2004. Regulation of CX3CL1/fractalkine expression in endothelial cells. *J. Atheroscler. Thromb.* 11: 15–21.
21. Fujimoto, K., T. Imaizumi, H. Yoshida, S. Takanashi, K. Okumura, and K. Satoh. 2001. Interferon-γ stimulates fractalkine expression in human bronchial epithelial cells and regulates mononuclear cell adherence. *Am. J. Respir. Cell Mol. Biol.* 25: 233–238.
22. Fong, A. M., L. A. Robinson, D. A. Steeber, T. F. Tedder, O. Yoshie, T. Imai, and D. D. Patel. 1998. Fractalkine and CX3CR1 mediate a novel mechanism of leukocyte capture, firm adhesion, and activation under physiologic flow. *J. Exp. Med.* 188: 1413–1419.
23. Umehara, H., E. T. Bloom, T. Okazaki, Y. Nagano, O. Yoshie, and T. Imai. 2004. Fractalkine in vascular biology: from basic research to clinical disease. *Arterioscler. Thromb. Vasc. Biol.* 24: 34–40.
24. Garton, K. J., P. J. Gough, C. P. Blobel, G. Murphy, D. R. Greaves, P. J. Dempsey, and E. W. Raines. 2001. Tumor necrosis factor-α-converting enzyme (ADAM17) mediates the cleavage and shedding of fractalkine (CX3CL1). *J. Biol. Chem.* 276: 37993–38001.
25. Hundhausen, C., D. Misztela, T. A. Berkhout, N. Broadway, P. Saftig, K. Reiss, D. Hartmann, F. Fahrenholz, R. Postina, V. Matthews, et al. 2003. The disintegrin-like metalloproteinase ADAM10 is involved in constitutive cleavage of CX3CL1 (fractalkine) and regulates CX3CL1-mediated cell-cell adhesion. *Blood* 102: 1186–1195.
26. Nanki, T., T. Imai, K. Nagasaka, Y. Urasaki, Y. Nonomura, K. Taniguchi, K. Hayashida, J. Hasegawa, O. Yoshie, and N. Miyasaka. 2002. Migration of CX3CR1-positive T cells producing type 1 cytokines and cytotoxic molecules into the synovium of patients with rheumatoid arthritis. *Arthritis Rheum.* 46: 2878–2883.
27. Nishimura, M., H. Umehara, T. Nakayama, O. Yoneda, K. Hieshima, M. Kakizaki, N. Dohmae, O. Yoshie, and T. Imai. 2002. Dual functions of fractalkine/CX3C ligand 1 in trafficking of perforin$^+$/granzyme B$^+$ cytotoxic effector lymphocytes that are defined by CX3CR1 expression. *J. Immunol.* 168: 6173–6180.
28. Imai, T., K. Hieshima, C. Haskell, M. Baba, M. Nagira, M. Nishimura, M. Kakizaki, S. Takagi, H. Nomiyama, T. J. Schall, et al. 1997. Identification and molecular characterization of fractalkine receptor CX3CR1, which mediates both leukocyte migration and adhesion. *Cell* 91: 521–530.
29. Combadiere, C., K. Salzwedel, E. D. Smith, H. L. Tiffany, E. A. Berger, and P. M. Murphy. 1998. Identification of CX3CR1: a chemotactic receptor for the human CX3C chemokine fractalkine and a fusion coreceptor for HIV-1. *J. Biol. Chem.* 273: 23799–23804.
30. Nanki, T., Y. Urasaki, T. Imai, M. Nishimura, K. Muramoto, T. Kubota, and N. Miyasaka. 2004. Inhibition of fractalkine ameliorates murine collagen-induced arthritis. *J. Immunol.* 173: 7010–7016.
31. Kojima, T., N. Tanuma, Y. Aikawa, T. Shin, A. Sasaki, and Y. Matsumoto. 1997. Myosin-induced autoimmune polymyositis in the rat. *J. Neurol. Sci.* 151: 141–148.
32. Livak, K. J., and T. D. Schmittgen. 2001. Analysis of relative gene expression data using real-time quantitative PCR and the 2(-DDC(T)) method. *Methods* 25: 402–408.
33. Gutala, R. V., and P. H. Reddy. 2004. The use of real-time PCR analysis in a gene expression study of Alzheimer's disease post-mortem brains. *J. Neurosci. Methods* 132: 101–107.
34. Dalakas, M. C. 2002. Muscle biopsy findings in inflammatory myopathies. *Rheum. Dis. Clin. North Am.* 28: 779–798.
35. Dalakas, M. C., and R. Hohlfeld. 2003. Polymyositis and dermatomyositis. *Lancet* 362: 971–982.
36. Ito, T., T. Kumamoto, H. Horinouchi, K. Yukishige, R. Sugihara, S. Fujimoto, and T. Tsuda. 2002. Adhesion molecule expression in experimental myositis. *Muscle Nerve* 25: 409–418.
37. Matsubara, S., T. Kitaguchi, A. Kawata, K. Miyamoto, H. Yagi, and S. Hirai. 2001. Experimental allergic myositis in SJL/J mouse: reappraisal of immune reaction based on changes after single immunization. *J. Neuroimmunol.* 119: 223–230.
38. Nemoto, H., K. Nemoto, H. Sugimoto, and M. Kinoshita. 2001. FK506 suppressed the inflammatory change of EAM in SJL/J mice. *J. Neurol. Sci.* 193: 7–11.

39. Rosenberg, N. L., S. P. Ringel, and B. L. Kotzin. 1987. Experimental autoimmune myositis in SJL/J mice. *Clin. Exp. Immunol.* 68: 117–129.
40. Matsubara, S., T. Shima, and M. Takamori. 1993. Experimental allergic myositis in SJL/J mice immunized with rabbit myosin B fraction: immunohistochemical analysis and transfer. *Acta Neuropathol. (Berl.)* 85: 138–144.
41. De Bleecker, J. L., V. I. Meire, W. Declercq, and E. H. Van Aken. 1999. Immunolocalization of tumor necrosis factor-α and its receptors in inflammatory myopathies. *Neuromuscul. Disord.* 9: 239–246.
42. Kalovidouris, A. E., and Z. Plotkin. 1995. Synergistic cytotoxic effect of interferon-γ and tumor necrosis factor-α on cultured human muscle cells. *J. Rheumatol.* 22: 1698–1703.
43. Shelton, G. D., N. A. Calcutt, R. S. Garrett, D. Gu, N. Sarvetnick, W. M. Campana, and H. C. Powell. 1999. Necrotizing myopathy induced by overexpression of interferon-γ in transgenic mice. *Muscle Nerve* 22: 156–165.
44. Kuru, S., A. Inukai, Y. Liang, M. Doyu, A. Takano, and G. Sobue. 2000. Tumor necrosis factor-α expression in muscles of polymyositis and dermatomyositis. *Acta Neuropathol. (Berl.)* 99: 585–588.
45. Sawai, H., Y. W. Park, J. Roberson, T. Imai, J. J. Goronzy, and C. M. Weyand. 2005. T cell costimulation by fractalkine-expressing synoviocytes in rheumatoid arthritis. *Arthritis Rheum.* 52: 1392–1401.
46. Ancuta, P., R. Rao, A. Moses, A. Mehle, S. K. Shaw, F. W. Luscinskas, and D. Gabuzda. 2003. Fractalkine preferentially mediates arrest and migration of $CD16^+$ monocytes. *J. Exp. Med.* 197: 1701–1707.
47. Thieblemont, N., L. Weiss, H. M. Sadeghi, C. Estcourt, and N. Haeffner-Cavaillon. 1995. $CD14^{low}CD16^{high}$: a cytokine-producing monocyte subset which expands during human immunodeficiency virus infection. *Eur. J. Immunol.* 25: 3418–3424.
48. Belge, K. U., F. Dayyani, A. Horelt, M. Siedlar, M. Frankenberger, B. Frankenberger, T. Espevik, and L. Ziegler-Heitbrock. 2002. The proinflammatory $CD14^+CD16^+DR^{++}$ monocytes are a major source of TNF. *J. Immunol.* 168: 3536–3542.
49. Feng, L., S. Chen, G. E. Garcia, Y. Xia, M. A. Siani, P. Botti, C. B. Wilson, J. K. Harrison, and K. B. Bacon. 1999. Prevention of crescentic glomerulonephritis by immunoneutralization of the fractalkine receptor CX3CR1 rapid communication. *Kidney Int.* 56: 612–620.
50. Lesnik, P., C. A. Haskell, and I. F. Charo. 2003. Decreased atherosclerosis in $CX3CR1^{-/-}$ mice reveals a role for fractalkine in atherogenesis. *J. Clin. Invest.* 111: 333–340.
51. Combadiere, C., S. Potteaux, J. L. Gao, B. Esposito, S. Casanova, E. J. Lee, P. Debre, A. Tedgui, P. M. Murphy, and Z. Mallat. 2003. Decreased atherosclerotic lesion formation in CX3CR1/apolipoprotein E double knockout mice. *Circulation* 107: 1009–1016.

STEM CELLS

EMBRYONIC STEM CELLS

Genetically Manipulated Human Embryonic Stem Cell-Derived Dendritic Cells with Immune Regulatory Function

SATORU SENJU,[a] HIROFUMI SUEMORI,[b] HITOSHI ZEMBUTSU,[c] YASUSHI UEMURA,[a] SHINYA HIRATA,[a] DAIKI FUKUMA,[a] HIDETAKE MATSUYOSHI,[a] MANAMI SHIMOMURA,[a] MIWA HARUTA,[a] SATOSHI FUKUSHIMA,[a] YUSUKE MATSUNAGA,[a] TOYOMASA KATAGIRI,[c] YUSUKE NAKAMURA,[c] MASATAKA FURUYA,[b] NORIO NAKATSUJI,[d] YASUHARU NISHIMURA[a]

[a]Department of Immunogenetics, Graduate School of Medical and Pharmaceutical Sciences, Kumamoto University, Kumamoto, Japan; [b]Laboratory of Embryonic Stem Cell Research, Stem Cell Research Center, Institute for Frontier Medical Sciences, Kyoto University, Kyoto, Japan; [c]Laboratory of Molecular Medicine, Human Genome Center, Institute of Medical Science, University of Tokyo, Tokyo, Japan; [d]Department of Development and Differentiation, Institute for Frontier Medical Sciences, Kyoto University, Kyoto, Japan

Key Words. Dendritic cells • Embryonic stem cells • Cell differentiation • Cell therapy

ABSTRACT

Genetically manipulated dendritic cells (DC) are considered to be a promising means for antigen-specific immune therapy. This study reports the generation, characterization, and genetic modification of DC derived from human embryonic stem (ES) cells. The human ES cell-derived DC (ES-DC) expressed surface molecules typically expressed by DC and had the capacities to stimulate allogeneic T lymphocytes and to process and present protein antigen in the context of histocompatibility leukocyte antigen (HLA) class II molecule. Genetic modification of human ES-DC can be accomplished without the use of viral vectors, by the introduction of expression vector plasmids into undifferentiated ES cells by electroporation and subsequent induction of differentiation of the transfectant ES cell clones to ES-DC. ES-DC introduced with invariant chain-based antigen-presenting vectors by this procedure stimulated HLA-DR-restricted antigen-specific T cells in the absence of exogenous antigen. Forced expression of programmed death-1-ligand-1 in ES-DC resulted in the reduction of the proliferative response of allogeneic T cells cocultured with the ES-DC. Generation and genetic modification of ES-DC from nonhuman primate (cynomolgus monkey) ES cells was also achieved by the currently established method. ES-DC technology is therefore considered to be a novel means for immune therapy. STEM CELLS *2007;25:2720–2729*

Disclosure of potential conflicts of interest is found at the end of this article.

INTRODUCTION

Embryonic stem (ES) cells are characterized by pluripotency and infinite propagation capacity, and the methods for genetic modification of ES cells, including targeted gene modification, have been well-established. This laboratory and others have devised methods to generate dendritic cells (DC) in vitro from mouse ES cells [1, 2]. The functions of mouse ES cell-derived DC (ES-DC), including stimulation of allogeneic T cells, processing and presentation of antigenic proteins, and migration upon in vivo transfer, are comparable to those of DC generated in vitro from bone marrow cells [3]. This laboratory has also established a strategy for the genetic modification of mouse ES-DC [1]. Expression vectors were introduced into ES cells by electroporation, and subsequently the transfectant ES cell clones were induced to differentiate to ES-DC. Studies using mice have demonstrated that in vivo transfer of genetically engineered mouse ES-DC is very useful for modulating immune responses both positively and negatively. It is possible to induce anticancer immunity [3–6] and prevent autoimmune disease [7, 8] in mouse models with genetically engineered ES-DC.

In the present study, looking toward future clinical application of ES-DC technology, a method was developed to generate ES-DC from human ES cells. The morphology and the results of functional and flow cytometric analyses indicate that human ES-DC possess the characteristic features of DC. cDNA microarray analysis revealed that the change of gene expression profile during generation and maturation of human ES-DC partially mimics that of monocyte-derived DC (Mo-DC). The currently established method was also applicable to cynomolgus monkey (*Macaca fascicularis*) ES cells.

MATERIALS AND METHODS

Cell Lines, Cytokines, and Reagents

The use of human ES cells was done in accordance with the Guidelines for Derivation and Utilization of Human Embryonic Stem Cells (2001) of the Ministry of Education, Culture, Sports, Science and Technology (MEXT), Japan, after approval by the Institutional Review Board. The human ES cell lines KhES-1 and KhES-3 have recently been established and maintained on mouse

Correspondence: Satoru Senju, M.D., Ph.D., Department of Immunogenetics, Graduate School of Medical and Pharmaceutical Sciences, Kumamoto University, 1-1-1 Honjo, Kumamoto 860-8556, Japan. Telephone: 81-96-373-5313; Fax: 81-96-373-5314; e-mail: senjusat@gpo.kumamoto-u.ac.jp Received April 30, 2007; accepted for publication July 27, 2007; first published online in STEM CELLS *EXPRESS* August 9, 2007. 1066-5099/2007/$30.00/0 doi: 10.1634/stemcells.2007-0321

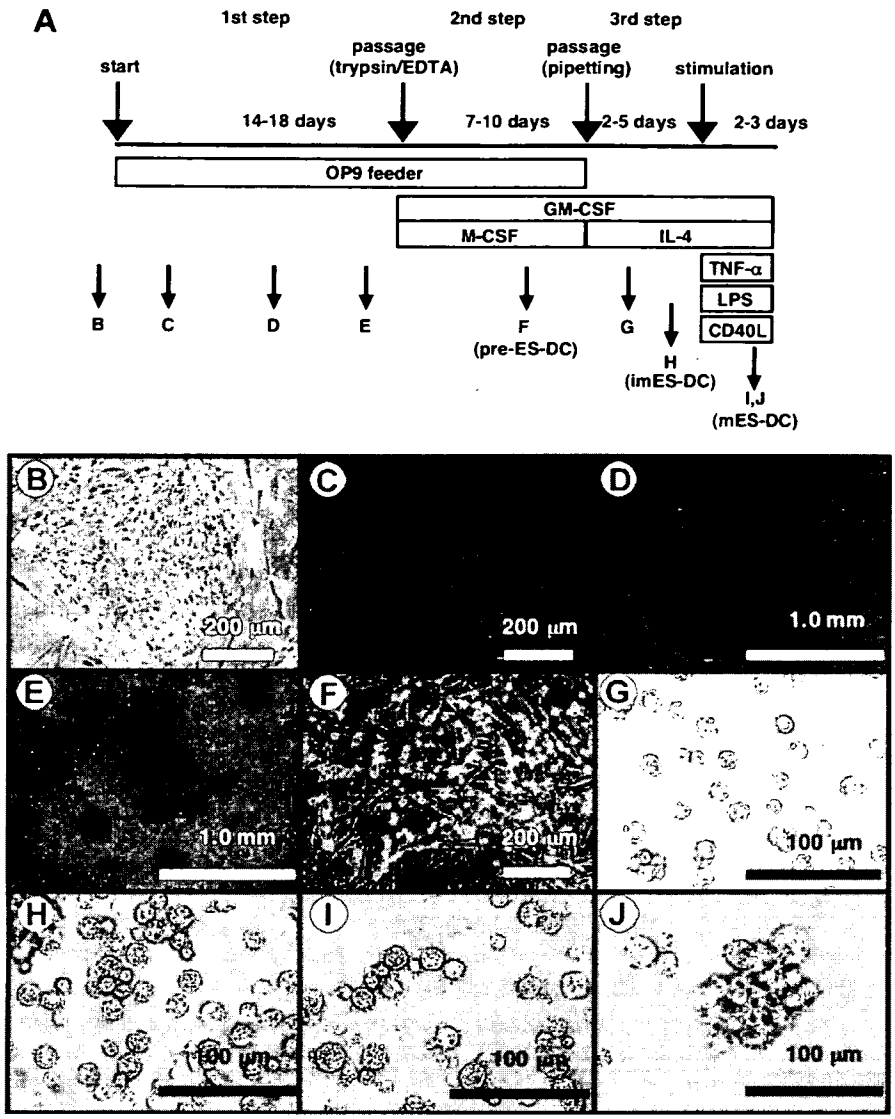

Figure 1. Culture protocol and morphological changes of human embryonic stem (ES) cell-derived cells during differentiation culture. **(A):** The schedule for the culture to induce differentiation of human ES cells into ES-DC is schematically depicted. **(B):** Undifferentiated human ES cells on primary embryonic fibroblast feeder layer. **(C–E):** ES cell-derived cells on day 3 **(C)**, day 11 **(D)**, and day 15 **(E)** in the first step. **(F):** Cells on day 6 in the second step. **(G–J):** Cells on day 1 **(G)**, day 3 **(H)**, and day 6 **(I, J)** in the third step. Cells shown in **(I, J)** had been stimulated with TNF-α plus LPS for 2 days. Abbreviations: ES-DC, embryonic stem cell-derived dendritic cells; GM-CSF, granulocyte macrophage colony-stimulating factor; IL, interleukin; imES-DC, immature embryonic stem cell-derived dendritic cells; LPS, lipopolysaccharide; M-CSF, macrophage colony-stimulating factor; mES-DC, mature embryonic stem cell-derived dendritic cells; TNF-α, tumor necrosis factor α.

primary embryonic fibroblast (PEF) feeder layers as previously described [9, 10]. Mouse-derived hematopoietic stromal cell line OP9 was treated with mitomycin C (10 μg/ml) for 1 hour before plating onto gelatin-coated tissue culture dishes to make feeder cell layers. The establishment and maintenance of cynomolgus monkey ES cell line CMK6 was also reported [11, 12]. Recombinant human granulocyte macrophage colony-stimulating factor (GM-CSF), macrophage colony-stimulating factor (M-CSF), interleukin-4 (IL-4), tumor necrosis factor α (TNF-α), and soluble CD40-ligand were purchased from Peprotech (London, http://www.peprotech.com). Lipopolysaccharide (LPS) from *Escherichia coli* and OK-432 were purchased from Sigma-Aldrich (St. Louis, http://www.sigmaaldrich.com) and Chugai Pharmaceutical (Tokyo, http://www.chugai-pharm.co.jp/hc/chugai_top_en.jsp), respectively.

Induction of Differentiation of ES Cells into ES-DC

The procedure for differentiation culture was composed of three steps (Fig. 1A). Step 1 was as follows: undifferentiated ES cells maintained on PEF were rinsed with phosphate-buffered saline (PBS) and treated with dissociation solution containing 1 mg/ml collagenase, 0.25% trypsin, and 20% knockout serum replacement (Invitrogen, Carlsbad, CA, http://www.invitrogen.com) in PBS [10] and cultured on OP9 feeder cell layers in minimum essential medium-α supplemented with 20% fetal calf serum (FCS) and 2-mercaptoethanol (50 μM). Culture of cells was continued for 14–18 days with human ES cells and for 11–13 days with cynomolgus monkey ES cells, and the medium was changed once every 3 days. At the end of this step, the cells were rinsed with PBS, treated with trypsin-EDTA (PBS containing 0.25% trypsin and 1 mM EDTA) for 30–40 minutes, and recovered. After resuspension in culture medium, the cells were plated onto culture dishes and incubated for 2–4 hours. Thereafter, floating or weakly adherent cells were recovered by pipetting, and any firmly adherent cells were discarded. Step 2 was as follows: after being passaged through nylon mesh (Cell Strainer 100 μm; BD Biosciences, Bedford, MA, http://www.bdbiosciences.com), cells recovered from one 90-mm dish were plated in two dishes with freshly prepared OP9 feeder layers. On the following day, the culture medium was exchanged with a medium containing GM-CSF (100 ng/ml) and M-CSF (50 ng/ml). The culture was continued for 7–10 days, depending on the propagation of floating cells on the feeder layers. Step 3 was as follows: ES cell-derived floating cells were recovered by pipetting; resuspended in RPMI 1640 medium containing 10% FCS, GM-CSF (100 ng/ml), and IL-4 (10 ng/ml); and cultured in Petri dishes ($3–5 \times 10^5$ cells per dish) without a feeder layer (Locus, Tokyo). To induce maturation, IL-4 (10 ng/ml), TNF-α (10 ng/ml), LPS (3 μg/ml), and, in some experiments, soluble CD40-ligand (20 ng/ml) or OK-432 (10 μg/ml) were simultaneously added on day 3 or 5 of this step, and the culture was continued for an additional 2–3 days. Differentiating cells were microscopically analyzed on an inverted microscope (IX70; Olympus, Tokyo, http://www.olympus-global.com).

Flow Cytometric Analysis

The following monoclonal antibodies (Ab) conjugated with fluorescein isothiocyanate or phycoerythrin were purchased from BD Pharmingen (San Diego, http://www.bdbiosciences.com/index_us.shtml) or eBioscience Inc. (San Diego, http://www.ebioscience.com): anti-human histocompatibility leukocyte antigen (HLA)-DR (clone L243, mouse IgG2a); anti-HLA-A, B, and C (clone G46–2.6, mouse IgG1); anti-human CD80 (clone L307.4, mouse IgG1); anti-human CD83 (clone HB15e, mouse IgG1); anti-human CD86 (clone FUN-1, mouse IgG1); anti-human CD40 (clone 5C3, mouse IgG1); anti-human B7-H1/programmed death-1-ligand-1 (PD-L1) (clone MIH1, mouse IgG1); and anti-human CD74 (clone M-B741, mouse IgG2a). As isotype-matched controls, mouse IgG2a (clone G155–178) and mouse IgG1 (clone MOPC-21) were used. The cell samples were treated with FcR-blocking reagent (Miltenyi Biotec, Bergisch Gladbach, Germany, http://www.miltenyibiotec.com) for 10 minutes, stained with the fluorochrome-conjugated Ab for 30 minutes, and washed three times with PBS/2% FCS. Intracellular staining with anti-CD74 monoclonal Ab was done by using IntraPrep (Beckman Coulter, Marseille, France, http://www.beckmancoulter.com). Stained cell samples were analyzed on a FACScan flow cytometer, and, in some experiments, the DC fraction was gated by forward and side scatters.

Enzyme-Linked Immunosorbent Assay to Detect Cytokine Production by ES-DC

Cells were cultured in 96-well flat-bottomed culture plates (1.2×10^5 cells in 150 μl of medium per well) in the presence or absence of soluble CD40-ligand, LPS, or OK432. After 60 hours of culture, supernatant was collected, and the concentration of TNF-α and IL-12 p70 was measured by using enzyme-linked immunosorbent assay (ELISA) kits (Pierce, Rockford, IL, http://www.piercenet.com).

Allogeneic T-Cell-Stimulation Assay

Mononuclear cells were isolated from heparinized peripheral blood of a human or a cynomolgus monkey housed in the Chemo-Sero-Therapeutic Research Institute (Kumamoto, Japan), using Ficoll-Paque PLUS (Amersham Biosciences, Uppsala, Sweden, http://www.amersham.com). T cells were purified using the Pan T cell isolation kit for humans or the kit for nonhuman primates (Miltenyi Biotec). The T cells (4×10^4/well) were cocultured with graded numbers of x-ray-irradiated (40 Gy) stimulator cells in RPMI 1640 medium supplemented with 10% human plasma in 96-well round-bottomed culture plates for 5 days. [^{3}H]-Methyl-thymidine (247.9 GBq/mmol) was added to the culture (0.037 MBq/well) for the last 16 hours. At the end this time, the cells were harvested onto glass fiber filters (PerkinElmer Life and Analytical Sciences, Boston, http://www.perkinelmer.com), and the incorporation of [^{3}H]-thymidine was measured by scintillation counting. In the experiment using PD-L1-transfectant ES-DC, anti-PD-L1 blocking Ab (clone MIH1; eBioscience) or control mouse IgG1 Ab (eBioscience) was added to the culture (10 μg/ml).

Recombinant Antigenic Protein

A DNA fragment encoding human glutamic acid decarboxylase (GAD65) p96–174 protein fragment was cloned into the prokaryotic expression vector pGEX-4T-3 (Amersham Biosciences), to generate a vector for glutathione *S*-transferase-fused GAD65 protein fragment (GST-GAD). The induction of the production of recombinant protein in *E. coli* (DH5α) and the extraction of the recombinant protein from bacterial inclusion bodies was done according to Frangioni and Neel [13]. The purification of the recombinant protein with glutathione-agarose (Sigma-Aldrich) was done as described in our previous report [14, 15]. The purity and integrity of the recombinant protein was confirmed by SDS-polyacrylamide gel electrophoresis. The protein was concentrated and separated from small peptide fragments, if any, with Centricon-10 (Millipore, Bedford, MA, http://www.millipore.com), and the solvent was changed from the elution buffer to the culture medium by dialysis.

Antigen Presentation Assay

A human CD4$^+$ T-cell clone, SA32.5, recognizing GAD65p111–131 in the context of HLA-DR53 molecule (DRA*0101+DRB4*0103) was established and maintained as previously described [16]. In the assay with the synthetic peptide, ES-DC stimulated with TNF-α (10 ng/ml) plus LPS (3 μg/ml) were harvested, incubated in the presence of peptide (6 μM) for 3 hours, washed four times with culture medium, and x-ray-irradiated (35 Gy). A T-cell proliferation assay was set up in a 96-well flat-bottomed culture plate with SA32.5 T cells (3×10^4 cells per well) and graded numbers of the peptide-loaded ES-DC in RPMI 1640 medium supplemented with 10% human plasma. In the assay with recombinant protein, the indicated amount of GST or GST-GAD protein was added to the coculture of SA32.5 T cells (3×10^4 cells per well) and irradiated ES-DC (1×10^4 cells per well). After 48 hours of culture, [^{3}H]-thymidine was added, and then after an additional 16 hours of culture, the cells were harvested and the incorporated radioactivity was counted.

Plasmid Construction

cDNA for human PD-L1 was isolated by polymerase chain reaction (PCR) with Pyrobest DNA polymerase (Takara, Osaka, Japan, http://www.takara.co.jp) using cDNA clone CS0DI011, purchased from Invitrogen (Carlsbad, CA, http://www.invitrogen.com), as a template. Double-stranded oligo DNA (5′-atgaacattttacttcagtatgtg-gtgaaaagtttcgat-3′) coding for GAD65p115–127 (the core epitope for SA32.5 T-cell clone) was ligated to human invariant chain (Ii)-based epitope presentation vector pCI [17] to generate GAD65-epitope-fused Ii. A cDNA fragment for HLA-DRB4*0103 was generated by reverse transcriptase (RT)-PCR from RNA isolated from peripheral blood mononuclear cells positive for *HLA-DRB4*0103*. The coding DNA fragments were cloned into a mammalian expression vector, pCAG-IRES-Neo, which is driven by the CAG promoter and includes an internal ribosomal entry site (IRES)-neomycin-resistance gene cassette [3].

Transfection of ES Cells

Human ES cells were harvested using CTK solution, dissociated into clusters of 50–100 cells by pipetting, and washed twice with Dulbecco's modified Eagle's medium (DMEM). The cells harvested from two 90-mm culture dishes with subconfluently growing ES cells were suspended in 0.1 ml of DMEM and mixed with 50 μg of linearized plasmid DNA dissolved in 0.1 ml of PBS in a 4-mm-gap cuvette. The electroporation of human ES cells was performed at 150 V and 200 μF on a Gene Pulser (Bio-Rad, Hercules, CA, http://www.bio-rad.com). The transfection of cynomolgus monkey ES cells was done as previously described [18], with some modifications. Cynomolgus monkey ES cells were harvested after treatment with trypsin-EDTA. ES cells ($1–1.5 \times 10^7$) suspended in 0.7 ml of DMEM were mixed with 50 μg of plasmid DNA in 0.1 ml of PBS in a 4-mm-gap cuvette. Electroporation was done at 250 V and 500 μF. After electroporation, the ES cells were cultured on G418-resistant PEF feeder layers in 90-mm culture dishes or six-well plates. Selection with G418 (150 μg/ml) was done from 2 to 4 days after the transfection, and G418-resistant ES cell colonies were picked up using a micropipette under microscopic observation on days 15–18 for human ES cells and on day 11 for monkey ES cells. The transfectant clones were transferred to 24-well culture plates with PEF and expanded in the presence of G418. ES cell transfectant clones with relatively high levels of expression of the transgene were selected on the basis of the resistance to a high dose (1–3 mg/ml) of G418 and the results of the RT-PCR analysis. Thereafter, the clones were subjected to the differentiation procedures. At the proper stages of differentiation, the cells were screened to select ES cell clones that highly expressed the transgene after differentiation, based on a flow cytometric analysis for PD-L1 and Ii transfectant human ES cells and on the antigen-presenting capacity for HLA-DRB4 transfectant cynomolgus monkey ES cells.

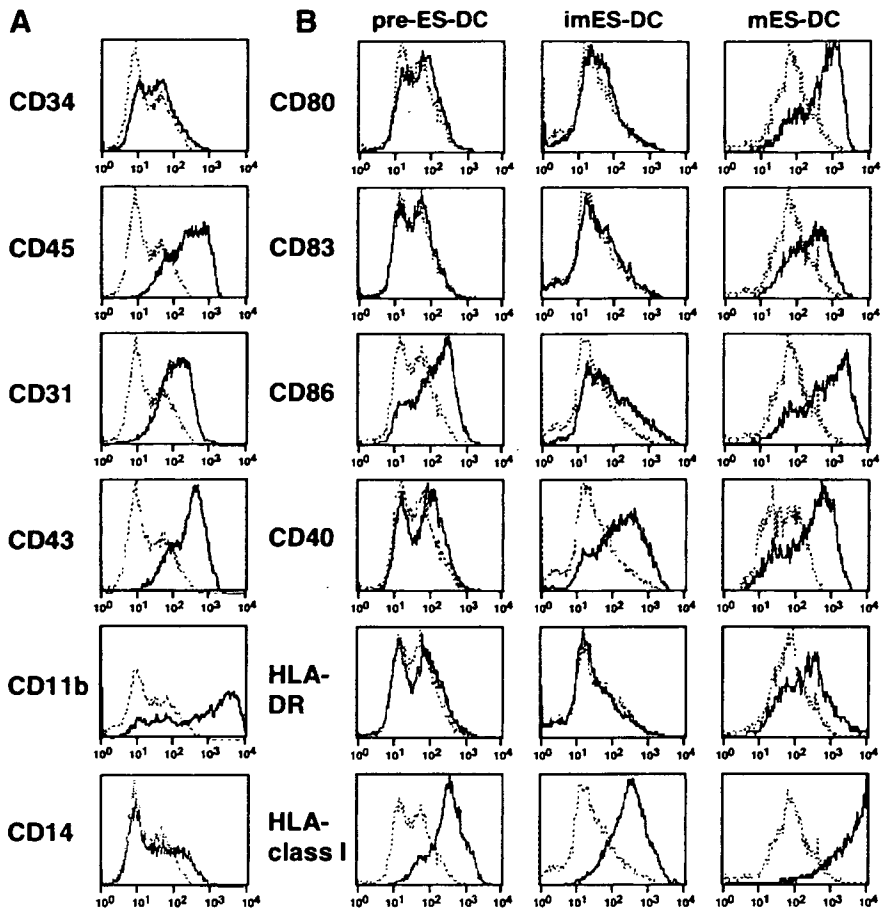

Figure 2. Cell surface phenotypes of human ES-DC. **(A):** ES cell-derived floating cells harvested on day 6 in the second step were analyzed for the cell surface expression of CD34, CD45, CD31, CD43, CD11b, and CD14. **(B):** ES cell-derived cells harvested on day 8 in the second step (pre-ES-DC) and from the third step before (imES-DC) and after (mES-DC) addition of maturation stimuli were analyzed for the cell surface expression of CD80, CD83, CD86, CD40, HLA-DR, and HLA class I. Staining profiles with specific antibody (Ab) (thick lines) and isotype-matched control Ab (thin, broken lines) are shown. Abbreviations: ES-DC, embryonic stem cell-derived dendritic cells; HLA, histocompatibility leukocyte antigen; imES-DC, immature embryonic stem cell-derived dendritic cells; mES-DC, mature embryonic stem cell-derived dendritic cells.

RT-PCR for Detection of the Transgene-Derived Transcripts

cDNA was synthesized from total cellular RNA with random hexamer primers and SuperScript II reverse transcriptase (Invitrogen). The following PCR primer sets were used: 5′-gctggattacatcaaagcactgaa-3′ and 5′-caacaaagtctggcttatatccaa-3′ for hypoxanthine-guanine phosphoribosyl transferase and 5′-ctgactgaccgcgttactcccaca-3′ and 5′-ttggttatagatgtatctgatcaggt-3′ for transgene-derived DRB4 transcript.

RESULTS

Differentiation of Human ES Cells to ES-DC

Based on previous experience in the generation of dendritic cells from mouse ES cells [1] and also based on the findings in a preliminary study using cynomolgus monkey ES cells, the feeder cell-coculture method was adopted for the generation of dendritic cells from human ES cells, instead of the embryoid body (EB)-based method. The human ES cell line selected was KhES-1; this line exhibited the highest growth rate among the three lines of human ES cell lines established in a recent study [9, 19]. For feeder cells, three lines of mouse stromal cell lines (ST2, OP9, and PA6) were evaluated for their capacity to induce hematopoietic differentiation of KhES-1 ES cells, and OP9 had the best yield among them (data not shown).

The protocol for the differentiation culture to generate ES-DC from human ES cells developed in the current study is composed of three steps, as shown in Figure 1A. At the beginning of the differentiation culture, undifferentiated ES cells maintained on mouse PEF feeders (Fig. 1B) were harvested using dissociation solution CTK [9] and plated on OP9 feeder cell layers (step 1). Next, the ES cells grew and formed clusters composed mostly of epithelial cell-like large flat cells (Fig. 1C, 1D). Clusters of round, cobblestone-like cells also appeared at approximately day 8, and those resembled the mesodermally differentiated cell clusters observed in hematopoietic differentiation culture of mouse ES cells [1, 20]. The size and number of round cell clusters gradually increased, and by around day 15, they covered 20%–30% of the surface area (Fig. 1E).

On days 15–18 of the first step, cells were recovered from the dishes using trypsin/EDTA and isolated nonadherent cells, and then they were seeded onto freshly prepared OP9 cell layers, to begin the second step. On the next day, the culture medium was exchanged for medium containing GM-CSF and M-CSF. Thereafter, small round cells, floating or loosely adhering to the feeder layer, appeared and gradually increased in number (Fig. 1F). The growth of the round cells depended primarily upon GM-CSF, thus suggesting that they grew in response to that factor. The cells were recovered and analyzed for their expression of hematopoietic cell lineage markers by flow cytometry (Fig. 2A). The cells expressed CD34 and CD45, thus indicating that they followed a hematopoietic cell lineage. They also expressed CD31, CD43, and CD11b, thus collectively indicating a commitment to a myeloid cell lineage. The double peaks seen in the histograms in Figure 2 reflect the heterogeneity of the analyzed cells in size and intensity of autofluorescence.

On days 7–10 of the second step, the floating or loosely adherent cells were harvested by pipetting and transferred to Petri dishes without feeder cells. We then cultured the cells in the presence of GM-CSF and IL-4 to start the third step. Following this passage, the cells changed their morphology from round to irregular shapes, and some had protrusions (Fig. 1G).

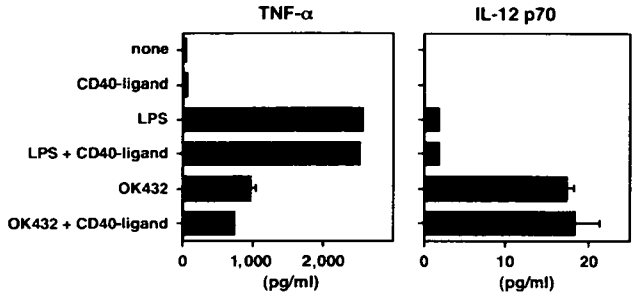

Figure 3. Production of TNF-α and IL-12 by embryonic stem cell-derived dendritic cells (ES-DC). ES-DC were recovered from the culture (third step, day 4) and replated (1.2×10^5 cells per 150 μl in 96-well culture plates) in the presence or absence of soluble CD40-ligand (20 ng/ml), LPS (3 μg/ml), or OK432 (10 μg/ml) as indicated. After 60 hours, supernatant was collected, and concentration of TNF-α and IL-12 p70 was measured by enzyme-linked immunosorbent assay. Data are indicated by mean value + SD of duplicate cultures. Abbreviations: IL, interleukin; LPS, lipopolysaccharide; TNF-α, tumor necrosis factor α.

Cells with protrusions gradually increased, and more than 50% of the cells exhibited DC-like irregular shapes after 2–3 days (Fig. 1H). The floating cells expressed CD86 and CD40 but scarcely expressed CD80 or CD83 (Fig. 2B). Expression of HLA-DR at this stage differed between experiments.

Figure 1I and 1J shows the cells after the simultaneous addition of TNF-α, LPS, soluble CD40-ligand, and IL-4. Generally, they exhibited longer protrusions than before the stimulation, and some of the protrusions were veil-like. Many of the cells formed aggregates. Flow cytometric analysis showed the increased expression of CD86 and the expression of CD80, CD83, and HLA-DR (Fig. 2B). Collectively, the cells exhibited the characteristics of DC in their morphology and expression of surface molecules, and thus they were designated human ES-DC.

Production of IL-12 and TNF-α by ES-DC was measured by ELISA (Fig. 3). Production of TNF-α was profoundly induced by either LPS or OK432. OK432, but not LPS, induced the production of IL-12, consistent with the reports that OK432 is an efficient inducer of IL-12 [21, 22]. Addition of CD40-ligand showed little effect on the production of these cytokines by human ES-DC.

ES cell-derived floating cells first appeared during the second step of the culture for differentiation (pre-ES-DC) and could readily be isolated by the pipetting procedure. Their morphology, pattern of expression of surface molecules, and T-cell-stimulation capacity (described below) continuously changed until the final maturation. To determine the change in gene expression associated with such changes in the phenotypes, the gene expression profiles of pre-ES-DC, immature ES-DC, and mature ES-DC were analyzed using cDNA microarrays. For reference purposes, human peripheral blood monocytes and immature and mature Mo-DC were also analyzed. The data for genes with relevance to immune functions were selected from the total microarray data and are shown in supplemental online Table 1. Consistent with the results of flow cytometric analysis (Fig. 2B), upregulation of the expression of genes encoding cell surface molecules such as HLA class I, HLA class II, CD86, and CD40, along with differentiation of ES-DC, was observed. In addition, expression of the genes related to DC function, including CD74/invariant chain, CCR7, and CCL17/TARC, was increased during the differentiation. Clustering analysis indicates similarity between change of the gene expression pattern from monocytes to immature Mo-DC and that from pre-ES-DC to immature ES-DC, as well as that from immature Mo-DC to mature Mo-DC and that from immature ES-DC to mature ES-DC (supplemental online Fig. 1).

The protocol of differentiation culture described thus far was originally developed using the KhES-1 line of human ES cells. This differentiation procedure was also applied to KhES-3, another human ES cell line. KhES-3 differentiation was similar to KhES-1 except that KhES-3 differentiated slightly more quickly than KhES-1, and a first-step culture of 14–15 days was sufficient for the differentiation of KhES-3.

Function of Human ES-DC

The capacity of the human ES-DC to stimulate T cells was examined based on the proliferative response of allogeneic T cells cocultured with ES-DC (Fig. 4A). ES cell-derived floating cells recovered from the second step (pre-ES-DC) showed little capacity to induce a response of T cells. In contrast, ES-DC following the third step before the addition of maturation stimuli (immature ES-DC) showed a weak but definite stimulation, and following exposure to the maturation stimuli (mature ES-DC) they showed a strong capacity to stimulate allogeneic T cells to proliferate.

Next, the antigen-presenting capacity of ES-DC was examined. KhES-1 is positive for the *HLA-DRB4*0103* gene encoding the β chain of HLA-DR53 molecule. Presumably, ES-DC derived from KhES-1 should express the DR53 molecule, and their ability to present antigen to DR53-restricted $CD4^+$ T cells was determined. As shown in Figure 4B, KhES-1-derived ES-DC preloaded with GAD65-derived synthetic peptide stimulated GAD65-specific DR53-restricted human T-cell clone SA32.5 to proliferate. To examine the capacity to process antigenic protein and present epitope, recombinant protein was used as the antigen (Fig. 4C). The SA32.5 T-cell clone cocultured with the ES-DC in the presence of recombinant GAD65 protein also showed a proliferative response, thus indicating that ES-DC processed the antigenic protein and presented the epitope derived from the protein in the context of HLA class II molecules.

Genetic Modification of Human ES-DC

Previous research established a strategy for the genetic modification of mouse ES-DC [1]. Briefly, the expression vectors were introduced into ES cells by electroporation, and subsequently the transfectant ES cell clones were induced to differentiate to ES-DC. The following experiments were performed to determine whether or not this strategy could be applicable to human ES cells.

PD-L1/B7-H1 is known to downmodulate responses of T cells upon interaction with the ligand, PD-1 on T cells [23]. An expression vector for human PD-L1 was introduced to KhES-1 by electroporation. The expression vector used was pCAG-INeo, driven by the CAG promoter and containing an IRES-neomycin-resistance gene cassette (Fig. 5A). Among the transfectant clones, 23 ES cell clones showing resistance to high does of G418 (2 mg/ml) were selected and subjected to the ES-DC-differentiation culture.

The expression of PD-L1 of the transfectant clones was examined by a flow cytometric analysis at the stage of immature ES-DC, harvested on day 2 of the third step of the differentiation culture. Although even nontransfectant ES-DC evidently expressed PD-L1 after maturation (data not shown), only a small population of them expressed PD-L1 at this stage (Fig. 5B, K1ES-DC). On the basis of the results of the analysis, one transfectant clone, KhES1-PD28, expressing the highest level of PD-L1 after the differentiation into immature ES-DC, was selected (Fig. 5B). Allogeneic T cells cocultured with immature ES-DC-PD28 showed a significantly lower response than those cocultured with nontransfectant immature ES-DC ($p < .05$; Fig.

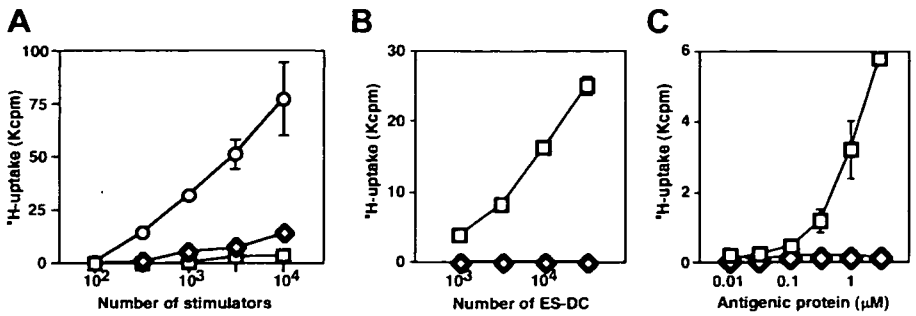

Figure 4. Stimulation of allogeneic T cells and antigen presentation by human ES-DC. **(A):** The indicated numbers of mature ES-DC (circles), immature ES-DC (diamonds), and pre-ES-DC (squares) were x-ray-irradiated (40 Gy) and cocultured with allogeneic human peripheral blood T cells (4×10^4 cells per well) in a 96-well round-bottomed culture plate for 5 days. Proliferation of T cells in the last 16 hours of the culture was measured based on [^{3}H]-thymidine uptake. The data are indicated as the mean value ± SD of duplicate cultures. **(B):** The indicated numbers of KhES-1-derived mature ES-DC prepulsed with glutamic acid decarboxylase (GAD) $65_{111-131}$ peptide (squares) and those left unpulsed (diamonds) were cocultured with a GAD65-specific, HLA-DR53-restricted human CD4$^+$ T-cell clone, SA32.5 (3×10^4 T cells per well) for 3 days. Proliferation of the T cells in the last 16 hours of the culture was measured by [^{3}H]-thymidine uptake. **(C):** Mature KhES-1-derived ES-DC (1×10^4 cells per well) were cocultured with SA32.5 T cells (3×10^4 cells per well) in the presence of the indicated concentrations of glutathione *S*-transferase (GST)-GAD65 recombinant protein (squares) or GST protein (diamonds) for 3 days. Proliferation of the T cells in the last 16 hours of the culture was measured by [^{3}H]-thymidine uptake. Abbreviation: ES-DC, embryonic stem cell-derived dendritic cells.

5C). The proliferation-reducing effect of the transgene-derived PD-L1 was abrogated by the addition of anti-PD-L1 blocking Ab ($p < .01$), ruling out the possibility that the introduction of the PD-L1 expression vector impaired the differentiation of ES-DC. Collectively, these results suggest that forced expression of PD-L1 on ES-DC downmodulated the proliferative response of cocultured allogeneic T cells via the interaction of PD-L1 with PD-1 on the T cells.

ES-DC carrying an epitope-presenting vector and expressing recombinant human invariant chain (Ii/CD74), which included GAD65p115–127 in the class II-associated invariant chain peptide region, were also generated (Fig. 5D). It was expected that the epitope could be efficiently targeted to the major histocompatibility complex (MHC) class II pathway [17]. Using a protocol similar to that used for the generation of PD-L1 transfectants, the vector was introduced into KhES-1 ES cells, and a transfectant clone, KhES-1-Ii23, highly expressing transgene-derived recombinant CD74, was selected by a flow cytometric analysis at the pre-ES-DC stage. The expression of CD74 was detected even in the nontransfectant pre-ES-DC, reflecting intrinsic expression of CD74 (Fig. 5E). The transfectant exhibited an increased expression of CD74 in comparison to the nontransfectants, thus indicating additional expression of the molecule derived from the transgene. The ability of the transfectant ES-DC, ES-DC-Ii23, to stimulate the GAD epitope-specific T-cell clone SA32.5 in the absence of antigenic peptide or protein was next examined. As a result, ES-DC-Ii23 stimulated SA32.5 T cells and induced their proliferation, thus demonstrating functional expression of the epitope-presentation vector in the transfectant ES-DC (Fig. 5F). The in vivo transfer of ES-DC transfected with this antigen-presenting vector is therefore expected to be useful for controlling the immune response in an antigen-specific manner [7].

Generation and Genetic Modification of Cynomolgus Monkey ES-DC

The differentiation protocol established using human ES cells was then applied to nonhuman primate ES cells. An ES cell line derived from cynomolgus monkey, CMK6 [11], was subjected to the ES-DC differentiation culture. Following the transfer to OP9 feeder layers, CMK6 cells grew and differentiated more rapidly than did human ES cells KhES-1 and KhES-3. The optimal duration of the first step of the differentiation culture for CMK6 was 11–13 days, whereas the duration ranged from 14 to 18 days for human ES cells. Figure 6A–6C illustrates the morphological changes of CMK6-derived cells following the second step of the differentiation culture. The surface phenotypes of the CMK6-derived pre-ES-DC, immature ES-DC, and mature ES-DC were then analyzed by flow cytometry (Fig. 6D). The double peaks seen in the histograms in Figure 6D reflect the heterogeneity of the analyzed cells in size and intensity of autofluorescence. Cynomolgus monkey ES-DC had the capacity to stimulate allogeneic cynomolgus monkey T cells (Fig. 6E), as human ES-DC did.

The expression vector for *HLA-DRB4*0103* (Fig. 7A) was introduced to CMK6. An analysis of the partial nucleotide sequence of *DRA* (*CyLA-DRA*) gene of CMK6 showed that the predicted amino acid sequence of the CyLA-DRα chain is very similar to that of HLA-DRα, with only one amino acid difference in α1 domain (GenBank accession no. AY591919). This suggested that the transgene-derived HLA-DRβ chain could associate with the intrinsic CyLA-DRα chain expressed in cynomolgus ES-DC and present an antigen to human T cells. The expression of the transgene before and after the ES-DC differentiation was confirmed by an RT-PCR analysis (Fig. 7B). ES-DC derived from a transfectant ES cell clone, cES-53-23, were prepulsed with synthetic GAD65 peptide and cocultured with the HLA-DR53-restricted, GAD65-specific T-cell clone SA32.5. Figure 7C shows that the GAD65 peptide-pulsed transfectant ES-DC stimulated the T cells to proliferate. In contrast, ES-DC originating from parental ES cells prepulsed with the peptide could not stimulate the T-cell clone. In addition, DR53-transfectant cynomolgus ES-DC had the capacity to process and present a protein antigen to the T cells (Fig. 7D). These results demonstrate the antigen-processing and presenting capacity of cynomolgus ES-DC and also the functional expression of the transgene that had been introduced into the ES cells before the differentiation. Thus, the effect and safety of the immune therapy by the in vivo transfer of ES-DC can be examined by preclinical studies using cynomolgus monkeys.

DISCUSSION

To establish the current culture protocol, various culture conditions were tested. As feeder cell lines, three lines of mouse stromal cells, OP9, PA6, and ST2, were comparatively evaluated. As a result, the use of OP9 was thus observed to produce

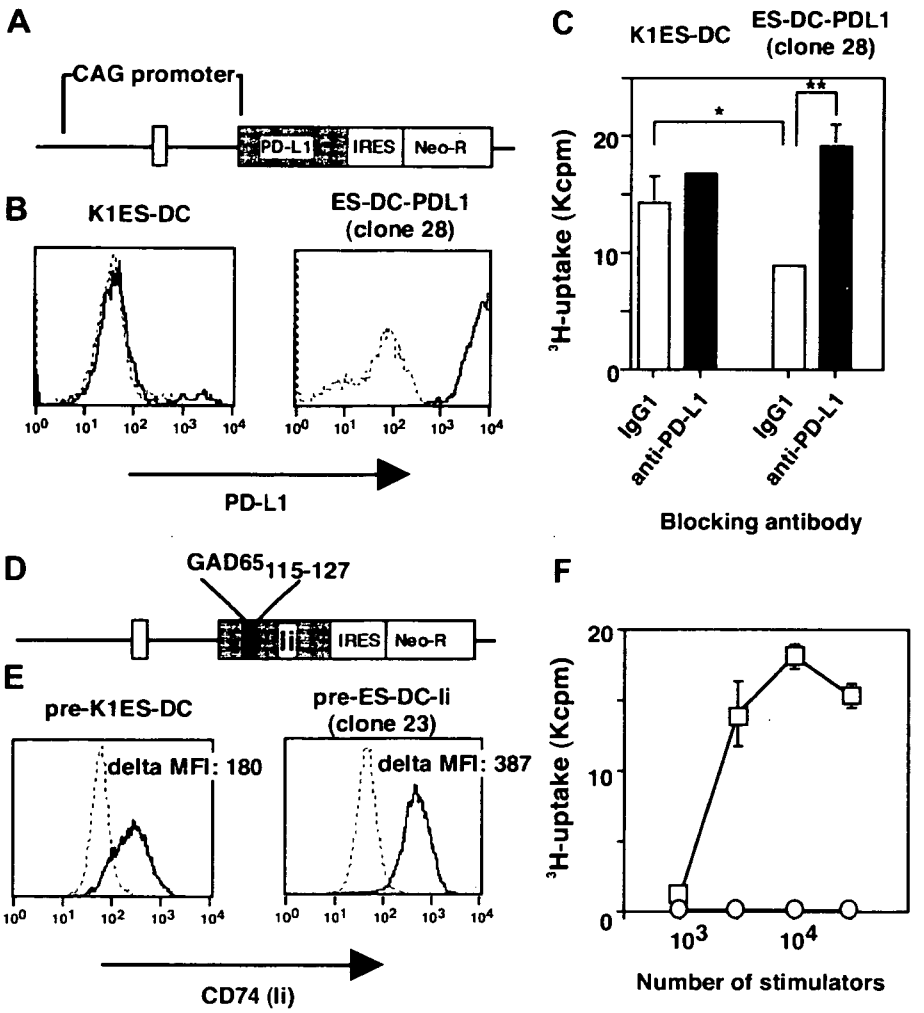

Figure 5. Genetic modification of human ES-DC. **(A):** Structure of the expression vector for human PD-L1. The expression of PD-L1 was driven by the CAG promoter, and the PD-L1-coding sequence was followed by IRES-neomycin-resistance gene (Neo-R), a selection marker. The open box in the CAG promoter indicates exon 1 of the rabbit β-actin gene contained in CAG promoter. **(B):** Transgene-derived PD-L1 expressed in immature ES-DC originated from transfectant embryonic stem (ES) cells was detected by flow cytometric analysis (ES-DC-PD-L1, clone 28). As a control, the staining profile of ES-DC derived from parental ES cell line (K1ES-DC) is shown. Specific stainings with anti-human-PD-L1 monoclonal antibody (Ab) (thick line) and isotype-matched control staining (thin, broken line) are shown. **(C):** The alloreactive response of T cells (4×10^4 cells per well) cocultured with immature ES-DC (1×10^4 cells per well) derived from the PD-L1-transfectant ES cells (ES-DC-PD-L1, clone 28) or those derived from parental ES cell line (K1ES-DC) is shown. The culture was done under the same conditions as those shown in Figure 3A except that anti-PD-L1 blocking Ab or isotype-matched mouse IgG1 was added to the culture. The statistical significance of the differences between the T-cell responses is indicated by asterisks (*, $p < .05$; **, $p < .01$). **(D):** Structure of expression vector for human Ii (Ii/CD74) including GAD65-derived epitope. The class II-associated invariant chain peptide region of the Ii-coding sequence was replaced with an oligo DNA-encoding $GAD65_{115-127}$. **(E):** Intracellular CD74 expressed in pre-ES-DC originated from transfectant ES cell clone (pre-ES-DC-human Ii [hIi], clone 23) and parental ES cell line (pre-K1ES-DC) was detected by a flow cytometric analysis. Specific staining with anti-human-CD74 monoclonal Ab (thick lines) and isotype-matched control staining (thin, broken lines) are shown. The values in the figure indicate the delta MFI between staining with the anti-CD74 and the isotype-matched control Ab. **(F):** SA32.5 T cells (3×10^4 cells per well) were cocultured with the indicated numbers of mature ES-DC-hIi clone 23 (squares) or nontransfectant ES-DC (circles) in the absence of exogenous antigen for 3 days. The proliferation of the T cells in the last 16 hours of the culture was measured by the [^{3}H]-thymidine uptake. Abbreviations: delta MFI, difference of mean fluorescence intensity; ES-DC, embryonic stem cell-derived dendritic cells; GAD, glutamic acid decarboxylase; Ii, invariant chain; IRES, internal ribosomal entry site.

the highest yield of ES-DC. Although ST2 also worked as feeder cells in the second step, the yield of ES-DC was approximately half of that obtained using OP9. It was also essential to remove any firmly adherent cells, when transferring the cells from the first to second step, by the procedure described in the Materials and Methods. At the end of the first step, many flat, adherent ES cell-derived cells were observed to form monolayers in the dishes. They probably differentiated into cell lineages other than mesoderm, and unless removed, they grew rapidly in the second step and inhibited the growth of hematopoietic cells.

Previously, two other groups reported the generation of functional antigen-presenting cells or DC from human ES cells. Zhan et al. adapted embryoid body-based induction of hematopoietic differentiation [24]. Slukvin et al. recently reported a method using OP9 [25]. Although there are some similarities between the method of Slukvin et al. [25] and the one reported here, the two methods differ in the following points.

In both methods, human ES cells were cocultured with OP9 feeder cells at the initial differentiation step (the first step). However, the duration of this culture step in our method (14–18 days) is significantly longer than the 10 days in the method of Slukvin et al. [25]. In our system, cells with morphology indicating mesodermal differentiation first appeared on day 8 or 9, and the extension of the first step of culture to days 14–18 significantly improved the yield of hematopoietically differentiated cells (Fig. 1D, 1E). In addition, we pretreated OP9 cells

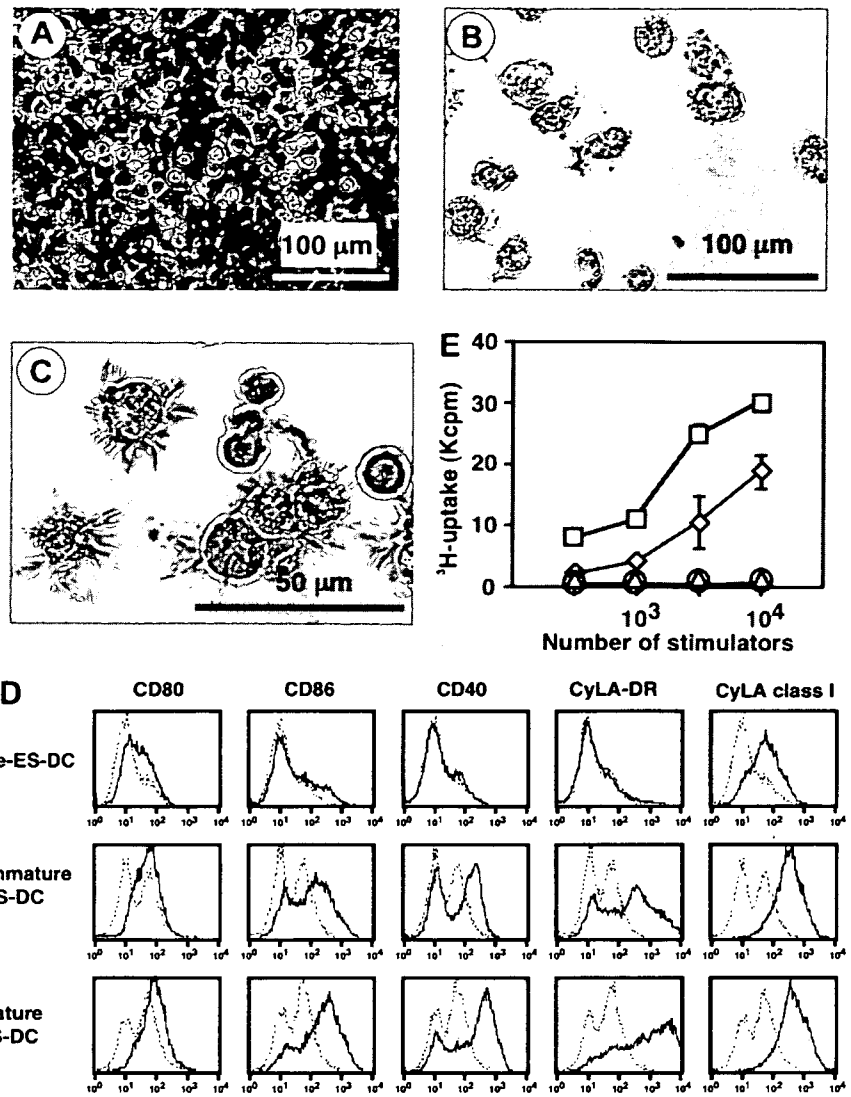

Figure 6. Generation of ES-DC from cynomolgus monkey embryonic stem (ES) cells. **(A–C):** The morphologies of cynomolgus monkey ES cell-derived differentiating cells (pre-ES-DC) at day 7 in the second step **(A)** and those in the third step before **(B)** and after **(C)** the addition of maturation stimuli are shown. **(D):** Cynomolgus monkey ES cell-derived cells harvested on day 8 in the second step (pre ES-DC) and from the third step before (immature ES-DC) and after (mature ES-DC) addition of maturation stimuli were analyzed for the cell surface expression of CD80, CD86, CD40, CyLA-DR, and CyLA class I. Staining patterns with specific monoclonal antibody (thick lines) and isotype-matched controls (thin, broken lines) are shown. **(E):** The indicated numbers of mature ES-DC (squares), immature ES-DC (diamonds), pre-ES-DC (circles), and undifferentiated cynomolgus ES cells (triangles) were x-ray-irradiated (40 Gy) and cocultured with allogeneic cynomolgus monkey peripheral blood T cells (4×10^4 cells per well) in a 96-well round-bottomed culture plate for 5 days. The proliferative responses of T cells in the last 16 hours of the culture were measured based on the [^{3}H]-thymidine uptake. Abbreviation: ES-DC, embryonic stem cell-derived dendritic cells.

with mitomycin C before use as feeder cells, and this was essential for efficient generation of hematopoietic cells. Treatment with mitomycin C may not only inactivate the mitosis of OP9 but also enhance the capacity of OP9 to support hematopoietic differentiation [26].

In the method of Slukvin et al., cells harvested from the first step of culture were directly transferred to 2-hydroxyethyl methacrylate-coated culture containers for the second step of culture [25]. In our method, cells harvested from the first step of culture were incubated in tissue culture-coated dishes for 2–5 hours to remove adherent cells. Removal of cells committed to nonmesodermal lineages by this procedure is essential. In addition, the second step of culture was also done with OP9 feeder in our method.

After the second step of culture, removal of dead cells and aggregated cells may be necessary in the method of Slukvin et al., as described in their report [25]. Indeed, we observed many dead cells, as well as DC-like cells, when we tried that method. In our method, most of recovered cells after the second step were viable, and removal of dead cells was not necessary.

The issues of safety and efficacy are critical for the establishment of ES-DC therapy. It is presumed that preclinical in vivo studies with the nonhuman primates will be required. Therefore, the ability to generate ES-DC from cynomolgus monkey ES cells is also considered to be important. It is probable that ES-DC can be generated from the ES cells of other nonhuman primates used in medical research, such as the rhesus monkey (*Macaca mulatta*) [27] and the common marmoset (*Callithrix jacchus*) [28]. For clinical application of the ES-DC technology, development of a feeder-free differentiation method may be required. Embryoid body-mediated differentiation methods may be one way to resolve this issue. In the mouse system, induction of mesodermal differentiation of ES cells using type IV collagen-coated culture plates has been reported [29, 30]. Several molecules have been reported to be involved in support of hematopoietic cell growth or differentiation by stromal cells [31–33]. Information on the molecular basis of the interaction between differentiating ES cells and feeder cells is valuable for the development of a feeder-free differentiation system.

Considering clinical applications, manipulation of function of ES-DC by genetic modification without use of viral vectors, demonstrated in the present study, has a significant advantage. However, random integration of multiple copies of transgenes into various genomic loci of ES cells is accompanied by risks such as activation of cellular oncogenes. Thus, a method to integrate transgenes into intended loci of the genome of human ES cells needs to be established.

Previously, we demonstrated a method for efficient targeted integration of expression vectors into specific genomic sites of mouse ES cells, using exchangeable gene-trap vector with Cre-

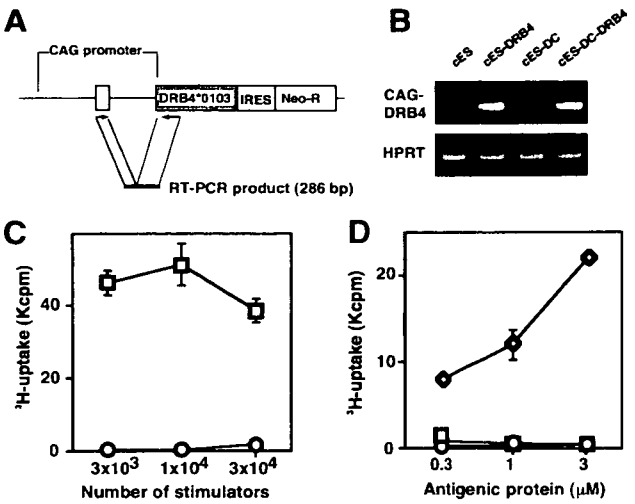

Figure 7. Antigen presentation to human T cells by genetically modified cES-DC. **(A):** The structure of HLA-DRB4*0103 expression vector is shown. The open box indicates the noncoding first exon of rabbit β-actin gene included in the CAG promoter. RT-PCR with PCR primers indicated by arrowheads generated PCR products of 286 base pairs from the transgene-derived mRNA. **(B):** Results of an RT-PCR analysis of parental cES and a transfectant embryonic stem cell clone (cES-DRB4) and derivative embryonic stem cell-derived dendritic cells (ES-DC) on the expression of transgene-derived mRNA (CAG-DRB4). The PCR products for HPRT transcript amplified from the same cDNA samples are also shown as control. **(C):** The indicated numbers of DRB4-transfectant ES-DC (squares) or nontransfectant ES-DC (circles) were preloaded with $GAD65_{111-131}$ peptide, x-ray-irradiated (40 Gy), and cocultured with SA32.5 T cells (3×10^4 cells per well) for 3 days. The proliferation of the T cells in the last 16 hours of the culture was measured by the [^{3}H]-thymidine uptake. **(D):** DRB4-transfectant ES-DC (diamonds) (1×10^4 cells per well) or nontransfectant ES-DC (squares) were cocultured with SA32.5 T cells (3×10^4 cells per well) in the presence of the indicated concentration of glutathione *S*-transferase (GST)-GAD recombinant protein for 3 days. DRB4-transfectant ES-DC and SA32.5 T cells were cocultured also in the presence of GST protein (circles). The proliferation of the T cells in the last 16 hours of the culture was measured by the [^{3}H]-thymidine uptake. Abbreviations: cES, cynomolgus embryonic stem cells; cES-DC, cynomolgus embryonic stem cell-derived dendritic cells; HPRT, hypoxanthine-guanine phosphoribosyl transferase; IRES, internal ribosomal entry site; RT-PCR, reverse transcriptase polymerase chain reaction.

Lox-mediated recombination system [1]. We are now trying to develop a system for targeted integration of transgenes into human ES cell genome. In this system, at first, gene-targeting vector conveying a drug resistance marker gene flanked by lox sequences is introduced, and then ES cell clones carrying the vector properly integrated by homologous recombination are selected. Subsequently, expression vectors with lox sequences are introduced with the aid of the Cre-Lox recombination system. Integration of a single copy of the transgene into the intended locus can be verified by Southern blot analysis. By this strategy, we can obtain ES cell clones with defined genetic modification, thus avoiding the risks accompanying the random integration of exogenous genes.

Allogenicity caused by differences in the genetic background between human ES cell lines and the recipients is considered to be a critical problem in medical application of ES-DC. We previously reported that mouse ES-DC administered into semiallogeneic recipients, sharing one MHC haplotype with the ES-DC, effectively primed antigen-specific cytotoxic T lymphocytes (CTL), suggesting that ES-DC can survive for a period long enough to stimulate antigen-specific CTL restricted by the shared MHC class I [4]. However, in the same semiallogeneic setting, we also observed five times that injection of no antigen-loaded ES-DC significantly reduced the efficiency of priming of antigen-specific CTL induced by the subsequent injection of antigen-loaded ES-DC (unpublished observations). Thus, repetitive stimulation with ES-DC expressing allogeneic MHC may result in activation and expansion of allogeneic MHC class I-reactive CTL, and in such recipients, subsequently transferred ES-DC may be rapidly eliminated. Repeated immunization may be required in clinical applications, for example, to induce antitumor immunity. Thus, we should resolve the problem of the histoincompatibilty between ES cell lines and recipients.

Methods for targeted gene modification of human ES cells and for targeted chromosome elimination of mouse ES cells have been developed [34–36]. To overcome the problem of histoincompatibility, genetic modification to inhibit expression of endogenous HLA class I in ES-DC may be effective. Deletion of more than 1,000 kilobases of entire HLA class I region of human ES cell genome by gene targeting is infeasible by currently available technology. However, disruption of the genes of molecules necessary for the cell surface expression of HLA class I molecules, such as transporter associated with antigen processing (TAP) or β2-microglobulin (β2M), is presumably feasible. In our plan, we will introduce expression vector encoding the β2M-linked form of recipient-matched HLA class I heavy chain into TAP1- or β2M-deficient human ES cells. We are now testing this strategy by using a mouse system.

ACKNOWLEDGMENTS

This work was supported in part by Grants-in-Aid 12213111, 14657082, 14570421, 14370115, 16590988, 17390292, 17015035, and 18014023 from MEXT, Japan; the Program of Founding Research Centers for Emerging and Reemerging Infectious Diseases launched as a project commissioned by MEXT, Japan; a Research Grant for Intractable Diseases from Ministry of Health and Welfare, Japan; Oncotherapy Science Inc. (to Y.Ni.); and grants from Japan Science and Technology Agency; the Tokyo Biochemical Research Foundation; Uehara Memorial Foundation; and Takeda Science Foundation. We thank Risa Goswammi for the cDNA microarray experiments, the Chemo-Sero-Therapeutic Research Institute for the cynomolgus monkey peripheral blood samples, and Tanabe Seiyaku Co., Ltd. for CMK6.

DISCLOSURE OF POTENTIAL CONFLICTS OF INTEREST

The authors indicate no potential conflicts of interest.

REFERENCES

1 Senju S, Hirata S, Matsuyoshi H et al. Generation and genetic modification of dendritic cells derived from mouse embryonic stem cells. Blood 2003;101:3501–3508.

2 Fairchild PJ, Brook FA, Gardner RL et al. Directed differentiation of dendritic cells from mouse embryonic stem cells. Curr Biol 2000;10: 1515–1518.

3 Matsuyoshi H, Senju S, Hirata S et al. Enhanced priming of antigen-specific CTLs in vivo by embryonic stem cell-derived dendritic cells expressing chemokine along with antigenic protein: Application to anti-tumor vaccination. J Immunol 2004;172:776–786.

4 Fukuma D, Matsuyoshi H, Hirata S et al. Cancer prevention with semi-

allogeneic ES cell-derived dendritic cells. Biochem Biophys Res Commun 2005;335:5–13.
5 Matsuyoshi H, Hirata S, Yoshitake Y et al. Therapeutic effect of alpha-galactosylceramide-loaded dendritic cells genetically engineered to express SLC/CCL21 along with tumor antigen against peritoneally disseminated tumor cells. Cancer Sci 2005;96:889–896.
6 Motomura Y, Senju S, Nakatsura T et al. Embryonic stem cell-derived dendritic cells expressing glypican-3, a recently identified oncofetal antigen, induce protective immunity against highly metastatic mouse melanoma, B16–F10. Cancer Res 2006;66:2414–2422.
7 Hirata S, Senju S, Matsuyoshi H et al. Prevention of experimental autoimmune encephalomyelitis by transfer of embryonic stem cell-derived dendritic cells expressing myelin oligodendrocyte glycoprotein peptide along with TRAIL or programmed death-1 ligand. J Immunol 2005;174:1888–1897.
8 Hirata S, Matsuyoshi H, Fukuma D et al. Involvement of regulatory T cells in the experimental autoimmune encephalomyelitis-preventive effect of dendritic cells expressing myelin oligodendrocyte glycoprotein plus TRAIL. J Immunol 2007;178:918–925.
9 Suemori H, Yasuchika K, Hasegawa K et al. Efficient establishment of human embryonic stem cell lines and long-term maintenance with stable karyotype by enzymatic bulk passage. Biochem Biophys Res Commun 2006;345:926–932.
10 Fujioka T, Yasuchika K, Nakamura Y et al. A simple and efficient cryopreservation method for primate embryonic stem cells. Int J Dev Biol 2004;48:1149–1154.
11 Suemori H, Tada T, Torii R et al. Establishment of embryonic stem cell lines from cynomolgus monkey blastocysts produced by IVF or ICSI. Dev Dyn 2001;222:273–279.
12 Suemori H, Nakatsuji N. Growth and differentiation of cynomolgus monkey ES cells. Methods Enzymol 2003;365:419–429.
13 Frangioni JV, Neel BG. Solubilization and purification of enzymatically active glutathione S-transferase (pGEX) fusion proteins. Anal Biochem 1993;210:179–187.
14 Uemura Y, Senju S, Maenaka K et al. Systematic analysis of the combinatorial nature of epitopes recognized by TCR leads to identification of mimicry epitopes for glutamic acid decarboxylase 65-specific TCRs. J Immunol 2003;170:947–960.
15 Fujita H, Senju S, Yokomizo H et al. Evidence that HLA class II-restricted human CD4+ T cells specific to p53 self peptides respond to p53 proteins of both wild and mutant forms. Eur J Immunol 1998;28:305–316.
16 Tabata H, Kanai T, Yoshizumi H et al. Characterization of self-glutamic acid decarboxylase 65-reactive CD4+ T-cell clones established from Japanese patients with insulin-dependent diabetes mellitus. Hum Immunol 1998;59:549–560.
17 Fujii S, Senju S, Chen YZ et al. The CLIP-substituted invariant chain efficiently targets an antigenic peptide to HLA class II pathway in L cells. Hum Immunol 1998;59:607–614.
18 Furuya M, Yasuchika K, Mizutani K et al. Electroporation of cynomolgus monkey embryonic stem cells. Genesis 2003;37:180–187.
19 Hasegawa K, Fujioka T, Nakamura Y et al. A method for the selection of human embryonic stem cell sublines with high replating efficiency after single-cell dissociation. STEM CELLS 2006;24:2649–2660.
20 Nakano T, Kodama H, Honjo T. Generation of lymphohematopoietic cells from embryonic stem cells in culture. Science 1994;265:1098–1101.
21 Itoh T, Ueda Y, Okugawa K et al. Streptococcal preparation OK432 promotes functional maturation of human monocyte-derived dendritic cells. Cancer Immunol Immunother 2003;52:207–214.
22 Nakahara S, Tsunoda T, Baba T et al. Dendritic cells stimulated with a bacterial product, OK-432, efficiently induce cytotoxic T lymphocytes specific to tumor rejection peptide. Cancer Res 2003;63:4112–4118.
23 Freeman GJ, Long AJ, Iwai Y et al. Engagement of the PD-1 immunoinhibitory receptor by a novel B7 family member leads to negative regulation of lymphocyte activation. J Exp Med 2000;192:1027–1034.
24 Zhan X, Dravid G, Ye Z et al. Functional antigen-presenting leucocytes derived from human embryonic stem cells in vitro. Lancet 2004;364:163–171.
25 Slukvin II, Vodyanik MA, Thomson JA et al. Directed differentiation of human embryonic stem cells into functional dendritic cells through the myeloid pathway. J Immunol 2006;176:2924–2932.
26 Zhang WJ, Park C, Arentson E et al. Modulation of hematopoietic and endothelial cell differentiation from mouse embryonic stem cells by different culture conditions. Blood 2005;105:111–114.
27 Thomson JA, Kalishman J, Golos TG et al. Isolation of a primate embryonic stem cell line. Proc Natl Acad Sci U S A 1995;92:7844–7848.
28 Sasaki E, Hanazawa K, Kurita R et al. Establishment of novel embryonic stem cell lines derived from the common marmoset (Callithrix jacchus). STEM CELLS 2005;23:1304–1313.
29 Nishikawa SI, Nishikawa S, Hirashima M et al. Progressive lineage analysis by cell sorting and culture identifies FLK1+VE-cadherin+ cells at a diverging point of endothelial and hemopoietic lineages. Development 1998;125:1747–1757.
30 Ogawa M, Kizumoto M, Nishikawa S et al. Expression of alpha4-integrin defines the earliest precursor of hematopoietic cell lineage diverged from endothelial cells. Blood 1999;93:1168–1177.
31 Ueno H, Sakita-Ishikawa M, Morikawa Y et al. A stromal cell-derived membrane protein that supports hematopoietic stem cells. Nat Immunol 2003;4:457–463.
32 Tian X, Morris JK, Linehan JL et al. Cytokine requirements differ for stroma and embryoid body-mediated hematopoiesis from human embryonic stem cells. Exp Hematol 2004;32:1000–1009.
33 Wang X, Hisha H, Taketani S et al. Neural cell adhesion molecule contributes to hemopoiesis-supporting capacity of stromal cell lines. STEM CELLS 2005;23:1389–1399.
34 Zwaka TP, Thomson JA. Homologous recombination in human embryonic stem cells. Nat Biotechnol 2003;21:319–321.
35 Urbach A, Schuldiner M, Benvenisty N. Modeling for Lesch-Nyhan disease by gene targeting in human embryonic stem cells. STEM CELLS 2004;22:635–641.
36 Matsumura H, Tada M, Otsuji T et al. Targeted chromosome elimination from ES-somatic hybrid cells. Nat Methods 2007;4:23–25.


See www.StemCells.com for supplemental material available online.

Regression of intestinal adenomas by vaccination with heat shock protein 105-pulsed bone marrow-derived dendritic cells in *Apc*$^{Min/+}$ mice

Kazunori Yokomine,[1,2] Tetsuya Nakatsura,[1,3] Satoru Senju,[1] Naomi Nakagata,[4] Motozumi Minohara,[5] Jun-ichi Kira,[5] Yutaka Motomura,[1,3] Tatsuko Kubo,[6] Yutaka Sasaki[2] and Yasuharu Nishimura[1,7]

Departments of [1]Immunogenetics and [2]Gastroenterology and Hepatology, Graduate School of Medical Sciences, Kumamoto University, 1-1-1 Honjo, Kumamoto 860-8556; [3]Immunotherapy Section, Investigative Treatment Division Research Center for Innovative Oncology, National Cancer Center Hospital East, 6-5-1 Kashiwanoha, Kashiwa 277-8577; [4]Center for Animal Resources and Development, Kumamoto University, 2-2-1 Honjo, Kumamoto 860-0811; [5]Department of Neurology, Neurological Institute, Graduate School of Medical Sciences, Kyushu University, 3-1-1 Maidashi, Higashi-ku, Fukuoka 812-8582; [6]Department of Molecular Pathology, Graduate School of Medical Sciences, Kumamoto University, 1-1-1 Honjo, Kumamoto 860-8556, Japan

(Received May 12, 2007/Revised August 6, 2007/Accepted August 7, 2007/Online publication September 24, 2007)

Heat shock protein (HSP) 105 is overexpressed in various cancers, but is expressed at low levels in many normal tissues, except for the testis. A vaccination with HSP105-pulsed bone marrow-derived dendritic cells (BM-DC) induced antitumor immunity without causing an autoimmune reaction in a mouse model. Because *Apc*$^{Min/+}$ mice develop multiple adenomas throughout the intestinal tract by 4 months of age, the mice provide a clinically relevant model of human intestinal tumor. In the present study, we investigated the efficacy of the HSP105-pulsed BM-DC vaccine on tumor regression in the *Apc*$^{Min/+}$ mouse. Western blot and immunohistochemical analyses revealed that the tumors of the *Apc*$^{Min/+}$ mice endogenously overexpressed HSP105. Immunization of the *Apc*$^{Min/+}$ mice with a HSP105-pulsed BM-DC vaccine at 6, 8, and 10 weeks of age significantly reduced the number of small-intestinal polyps accompanied by infiltration of both CD4$^+$ and CD8$^+$ T cells in the tumors. Cell depletion experiments proved that both CD4$^+$ and CD8$^+$ T cells play a critical role in the activation of antitumor immunity induced by these vaccinations. These findings indicate that the HSP105-pulsed BM-DC vaccine can provide potent immunotherapy for tumors that appear spontaneously as a result of the inactivation of a tumor suppressor gene, such as in the *Apc*$^{Min/+}$ mouse model. (*Cancer Sci* 2007; 98: 1930–1935)

Colorectal cancer is the third most common cancer and the fourth most frequent cause of cancer death worldwide. Every year, more than 945 000 people develop colorectal cancer worldwide, and approximately 492 000 patients die.[1] For patients with advanced stages of colorectal cancer, adjuvant systemic chemotherapy is a standard treatment. Major progress has been made by the introduction of regimens containing new cytotoxic drugs such as irinotecan and oxaliplatin; however, the new therapeutic regimens have led to only 8–9 months of progression-free survival.[2] Consequently, the development of new and effective therapeutic approaches, such as immunotherapy, is needed to expand treatment options.

The progression from normal epithelium to colorectal cancer is a multistep process involving the accumulation of multiple genetic alterations.[3] The *APC* gene, a tumor suppressor, is considered to be a gatekeeper in colon tumorigenesis,[4] and one of the earliest molecular events is the loss of function of the *APC* gene product.[5] APC forms a multimeric complex with the axis inhibition protein (AXIN)2 and glycogen synthase kinase 3β, which regulates the nuclear accumulation of β-catenin, a signal transducer of the wnt pathway.[6] When the APC–β-catenin complex is destabilized because of *APC* mutations, β-catenin binds and activates transcription factors that regulate the expression of potent oncogenes such as *c-Myc* and *c-Met*.[7] The importance of the *APC* gene product was confirmed by the demonstration that 80% of all sporadic colorectal cancers are characterized by one or more mutations in the *APC* gene, approximately 60% of which result in the expression of a truncated version of the APC protein.[8]

The *Apc*$^{Min/+}$ mouse has a nonsense mutation from T to A in the *Apc* gene at codon 850, homologous to the human germline and somatic *APC* mutation.[9] Although homozygous mice die before birth, all heterozygous mice develop multiple adenomas throughout their intestinal tract at an early age.[10] The *Apc*$^{Min/+}$ mouse model is unique in that tumors appear spontaneously in the intestinal tract, rather than as a result of induction by a carcinogen. This model is particularly advantageous for testing preventive agents targeted against early stage lesions because adenomas grow to a grossly detectable size within a few months on a defined genetic background.[10] Because *Apc*$^{Min/+}$ mice develop tumors due to the inactivation of the same tumor suppressor gene known to be involved in the pathogenesis of most colon cancers in humans, this model represents a clinically relevant model of human intestinal tumorigenesis.[10] Furthermore, germline mutations in the human *APC* gene cause FAP, whose symptoms resemble those of an *Apc*$^{Min/+}$ mouse. Therefore, this model provides useful information about not only colon cancer but also FAP.

Heat shock proteins are soluble intracellular proteins that are expressed ubiquitously, and their expression can be induced at much higher levels due to heat shock or other forms of stress. The essential functions of HSP are to bind and protect partially denatured proteins from further denaturation and aggregation.[11] A previous study reported that HSP105 (often called HSP110), identified with serological identification of antigens using the recombinant expression cloning (SEREX) method, is overexpressed in a variety of human cancers, including colorectal, pancreatic, thyroid, esophageal, and breast carcinoma, whereas HSP105 is expressed at lower levels in many normal tissues, except for the testis.[12,13] Immunotherapy targeted at HSP105 in the mouse prophylactic model, such as HSP105-pulsed BM-DC and *HSP105* DNA vaccines, induce antitumor immunity without causing an autoimmune reaction.[14,15] These findings indicate that HSP105 itself could be considered as a valuable tumor-associated antigen for immune-based treatment of various tumors.

[7]To whom correspondence should be addressed.
E-mail: mxnishim@gpo.kumamoto-u.ac.jp

Abbreviations: APC, adenomatous polyposis coli; BM-DC, bone marrow-derived dendritic cell; COX, cydooxygenase; DC, dendritic cell; ELISPOT, enzyme-linked immunospot; FAP, familial adenomatous polyposis; HSP, heat shock protein; mAb, monodonal antibody; MBP, myelin basic protein; MHC, major histocompatibility complex; PBS, phosphate-buffered saline.

doi: 10.1111/j.1349-7006.2007.00612.x

Another study reported that HSP105 is involved in tumorigenesis by protecting cancer cells from apoptosis.[16] The constitutive overexpression of HSP105 protein was found to be essential for various cancer cells to survive and, conversely, the apoptosis-inducing effect of HSP105 small interfering RNA (siRNA) is specific for cancer. In contrast, HSP can also stimulate an adaptive immune response against antigens bound to HSP,[17] provided that the vaccine forms a complex of recombinant HSP110 and target tumor-associated antigen.[18,19]

In the present study, $Apc^{Min/+}$ mice were used as a model of a cancer immunotherapy for human colorectal cancer. Because tumors in $Apc^{Min/+}$ mice strongly express HSP105, the efficacy of immunization with HSP105-pulsed BM-DC for preventing the development of tumors in $Apc^{Min/+}$ mice was investigated.

Materials and Methods

Mice and genotyping. Frozen embryos of $Apc^{Min/+}$ mice obtained from the Jackson Laboratory were transferred to C57BL/6J mice (purchased from Charles River Japan, Yokohama, Japan) at the Center for Animal Resources and Development, Kumamoto University. Mice at 4–5 weeks of age were characterized for the *Apc* genotype by polymerase chain reaction analysis of tail DNA with the use of allele-specific primers.[20] The concentrations of these primers were 1.0 μM (5′-TGAGAAAGACAGAAGTTA-3′), 1.0 μM (5′-TTCCACTTTGGCATAAGGC-3′), and 0.2 μM (5′-GCCATCCCTTCACGTTAG-3′). The amplification conditions were 5 min at 94°C before 35 cycles at 94°C for 1 min, 50°C for 1 min, and 72°C for 1 min, followed by a final extension at 72°C for 5 min. The mice were maintained by breeding male $Apc^{Min/+}$ mice to female C57BL/6J mice. The mice were kept under specific pathogen-free conditions and these experiments were approved by the Animal Research Committee of Kumamoto University.

Production of recombinant proteins. Highly purified recombinant mouse HSP105 was produced from *Escherichia coli* strain BL21 cells transduced with the mouse *HSP105* gene expression vector, as described previously.[14,21] We also produced highly purified recombinant MBP as a negative control, which was prepared from bacterial lysate in the same way as the preparation of recombinant HSP105. Both recombinant HSP105 and MBP were estimated to be almost endotoxin free using a Limulus amebocyte lysate assay kit (BioWhittaker, Walkersville, MD, USA), and the endotoxin contents in the materials were <10 endotoxin U/mg.

Immunizations and scoring of tumors. HSP105-pulsed BM-DC were prepared as described previously.[14,22] The mice were inoculated intraperitoneally with HSP105-pulsed BM-DC (5×10^5) suspended in 200 μL PBS at 6, 8, and 10 weeks of age. The mice were treated with BM-DC alone, MBP-pulsed BM-DC, or PBS as controls. At 12 weeks of age the mice were killed and their small intestines were removed and fixed with formaldehyde. The intestines were then opened and stained with methylene blue and the number of tumors was counted.

Western blot and immunohistochemical analysis. Western blotting and the immunohistochemical detection of HSP105 were carried out as described previously.[12,16] Rabbit polyclonal antihuman HSP105 (Santa Cruz Biotechnology, Santa Cruz, CA, USA) was used as the primary antibody in this study. The immunohistochemical staining of $CD4^+$ and $CD8^+$ T cells was carried out as described previously.[14] mAb specific to CD4 (L3T4; BD PharMingen, San Diego, CA, USA) and CD8 (Ly-2; BD PharMingen) were used for staining.

Depletion of $CD4^+$ or $CD8^+$ T cells in mice. Rat mAb GK1.5 specific to mouse CD4 and 2.43 specific to mouse CD8 were used to deplete $CD4^+$ and $CD8^+$ T cells, respectively, *in vivo*. The 6-week-old $Apc^{Min/+}$ mice were injected with ascites (500 μg/mouse) from hybridoma-bearing nude mice six times intraperitoneally with an interval of 3–4 days between injection. Normal rat IgG (Chemicon, Temecula, CA, USA) was used as a control. The depletion of T cell subsets was monitored by a flow cytometric analysis, which showed a more than 90% specific depletion in the number of splenocytes.

ELISPOT assay. The $Apc^{Min/+}$ mice were immunized with HSP105-pulsed BM-DC or BM-DC alone at 6 and 8 weeks of age. At 10 weeks of age, spleen cells were harvested and depleted of $CD4^+$ or $CD8^+$ T cells using a magnetic cell-sorting system with antimouse CD4 mAb and antimouse CD8a (Mittenyi Biotec GmbH, Bergisch Gladbach, Germany) mAb, respectively. The purity of these T-cell subsets exceeded 95% based on a flow cytometric analysis. $CD4^-$ T cells were used as a source of $CD8^+$ T cells and antigen-presenting cells, and $CD8^-$ T cells were used as a source of $CD4^+$ T cells and antigen-presenting cells. Five hundred thousand $CD4^-$ or $CD8^-$ T cells were added to each well in triplicate cultures of RPMI-1640 medium containing 10% fetal calf serum (FCS) together with 2 μg/mL HSP105, MBP, and one with medium only at 37°C for 24 h. Then ELISPOT assays were carried out as described previously.[12]

Statistical analysis. The statistical significance of differences between the experimental groups was determined using Student's *t*-test. The overall survival rate was calculated using the Kaplan–Meier method, and statistical significance was evaluated using Wilcoxon's test. A value of $P < 0.05$ was considered to be statistically significant.

Results

Overexpression of HSP105 in intestinal adenomas of the $Apc^{Min/+}$ mice. A previous study reported that mouse HSP105 is overexpressed in liver metastasis of a murine colorectal adenocarcinoma cell line (Colon26), and in lung metastasis of a murine melanoma cell line (B16-F10).[15] The expression of HSP105 in tumors of $Apc^{Min/+}$ mice were thereby analyzed. The small intestines of $Apc^{Min/+}$ mice were excised, and the expression level of HSP105 was evaluated by both western blot and immunohistochemical analyses. The $Apc^{Min/+}$ mice developed adenomatous polyps spontaneously, predominantly in and throughout the small intestine at 4 months of age (Fig. 1a). Both western blot and immunohistochemical analyses confirmed the strong expression of HSP105 in the tumors of $Apc^{Min/+}$ mice (Fig. 1b,c). Based on these observations, the $Apc^{Min/+}$ mouse was chosen as a murine model of cancer immunotherapy targeted at HSP105.

Immunization with HSP105-pulsed BM-DC vaccine reduced the number of small intestinal polyps in $Apc^{Min/+}$ mice. The preventive effects of HSP105-pulsed BM-DC vaccination on the development of adenomatous polyps in the $Apc^{Min/+}$ mice were investigated. The mice were divided into four groups consisting of 10 mice each, inoculated intraperitoneally with PBS (group 1), BM-DC (group 2), MBP-pulsed BM-DC (group 3), or HSP105-pulsed BM-DC (group 4) at 6, 8, and 10 weeks of age. Two weeks after the last immunization, the number of tumors in the small intestine was counted.

Tumors had already developed in the small intestine of $Apc^{Min/+}$ mice at the time of the first vaccination (6 weeks of age). Each mouse had a mean of 6.3 ± 3.4 tumors at that time. The mean number of tumors at 12 weeks of age was 20.9 ± 9.6 in group 4, which was significantly less ($P = 0.006$) than the numbers in group 1 (37.8 ± 11.0), group 2 (40.8 ± 11.0), and group 3 (34.8 ± 9.5) (Fig. 2a). It was therefore concluded that the HSP105-pulsed BM-DC vaccine has the potential to prevent the growth of tumors expressing HSP105. The survival time in group 4 (175.3 ± 32.6 days) tended to be longer than that in group 1 (146.7 ± 13.0 days) and in group 2 (152.7 ± 25.5 days); however, the difference between group 4 and group 2 was not statistically significant ($P = 0.081$; Fig. 2b). No apparent abnormalities, such as weight loss, hair abnormality, or paralysis, were observed in

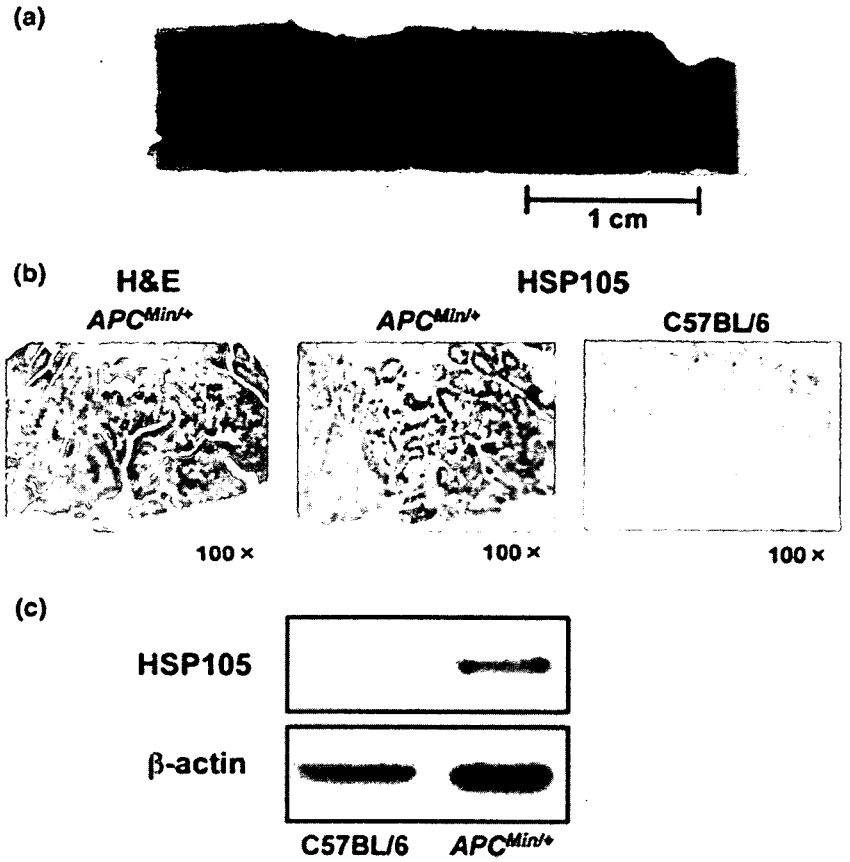

Fig. 1. Overexpression of heat shock protein (HSP) 105 in adenomatous polyps of $Apc^{Min/+}$ mice. (a) Macroscopic polyps in the small intestine of 4-month-old $Apc^{Min/+}$ mice. (b) A microscopic analysis of polyps in the small intestine of 12-week-old $Apc^{Min/+}$ mice stained with hematoxylin–eosin (left) and anti-HSP105 monoclonal antibody (middle). A normal small intestine was stained with anti-HSP105 monoclonal antibody as a negative control (right). Objective magnification was ×100. (c) Western blot analysis of HSP105 in the small intestine of 4-month-old $Apc^{Min/+}$ mice. The samples were small intestines of $Apc^{Min/+}$ and C57BL/6J mice homogenized in lysis buffer. The small intestines of three mice per group were pooled.

the mice immunized with HSP105-pulsed BM-DC, suggesting that serious autoimmunity was not observed in the mice. A histological analysis of the major organs (brain, lung, heart, liver, small intestine, kidney, and testis) of the immunized mice revealed no pathological inflammation (data not shown).

Both CD4⁺ and CD8⁺ T cells are required for antitumor immunity. To determine the role of $CD4^+$ and $CD8^+$ T cells in the reduction of tumor development in $Apc^{Min/+}$ mice immunized with HSP105-pulsed BM-DC, mice were depleted of $CD4^+$ or $CD8^+$ T cells by treatment with anti-CD4 or anti-CD8 mAb, respectively, *in vivo*. During the depletion procedure, the mice were immunized with PBS or HSP105-pulsed BM-DC vaccine (Fig. 3a). In the group of mice immunized with HSP105-pulsed BM-DC, together with inoculation of anti-CD4 mAb (35.5 ± 10.8) or anti-CD8 mAb (30.2 ± 9.6), the tumor numbers were significantly larger than those in the mice given rat IgG (18.8 ± 5.9) or left untreated (19.9 ± 7.7). The differences in the tumor numbers between the anti-CD4 mAb-treated group and the rat IgG-treated group ($P = 0.002$), and between the anti-CD8 mAb-treated group and the rat IgG-treated group ($P = 0.013$) were statistically significant. In the group of mice inoculated with PBS, the numbers of tumors in the mice given either anti-CD4 mAb (38.1 ± 5.7) or anti-CD8 mAb (38.1 ± 5.6) did not differ significantly from those in the mice given rat IgG (37.8 ± 4.8) or in the untreated mice (40.8 ± 6.1) (Fig. 3b). These results suggest that both $CD4^+$ and $CD8^+$ T cells play a crucial role in the protective antitumor immunity induced by the HSP105-pulsed BM-DC vaccine, because the HSP105-pulsed BM-DC vaccine was not effective in the mice showing a depletion of either $CD4^+$ or $CD8^+$ T cells.

Detection of HSP105-specific T cells in mice immunized with the HSP105-pulsed BM-DC vaccine. The $Apc^{Min/+}$ mice were immunized with HSP105-pulsed BM-DC or BM-DC at 6 and 8 weeks of age. At 10 weeks of age, spleen cells were harvested and depleted of $CD4^+$ or $CD8^+$ T cells using magnetic cell-sorting system, and the ELISPOT assay was carried out. The ELISPOT assay showed that the $CD8^-$ cells ($CD4^+$ T cells and antigen-presenting cells) derived from the mice immunized with HSP105-pulsed BM-DC produced a significantly larger amount of interferon-γ in response to HSP105 than did $CD8^-$ cells derived from mice immunized with BM-DC. Similar results were observed for the $CD4^-$ cells ($CD8^+$ T cells and antigen-presenting cells) (Fig. 4a). These observations clearly indicate that both HSP105-specific $CD4^+$ and $CD8^+$ T cells were induced in the mice immunized with HSP105-pulsed BM-DC vaccine.

To investigate the antitumor effect of the HSP105-pulsed BM-DC vaccination, the tumor was evaluated histopathologically. The small intestines derived from the mice used for the ELISPOT assay were stained with anti-CD4 or anti-CD8 mAb. Both $CD4^+$ and $CD8^+$ T cells infiltrated into the tumors of mice immunized with HSP105-pulsed BM-DC; however, this was not the case in tumors derived from the mice immunized with BM-DC (Fig. 4b). These results suggest that HSP105-pulsed BM-DC have the potential to sensitize many HSP105-specific $CD4^+$ and $CD8^+$ T cells to kill tumor cells.

Discussion

In the present study, the HSP105-pulsed BM-DC vaccine could sensitize HSP105-specific T cells *in vivo* and inhibited the spontaneous development of intestinal tumors overexpressing HSP105 in $Apc^{Min/+}$ mice. For diseases of germline mutations that cause malignancy throughout the body, such as FAP, novel strategies for the prevention of cancer are needed urgently because there is no satisfactory treatment for FAP. Therefore,

doi: 10.1111/j.1349-7006.2007.00612.x

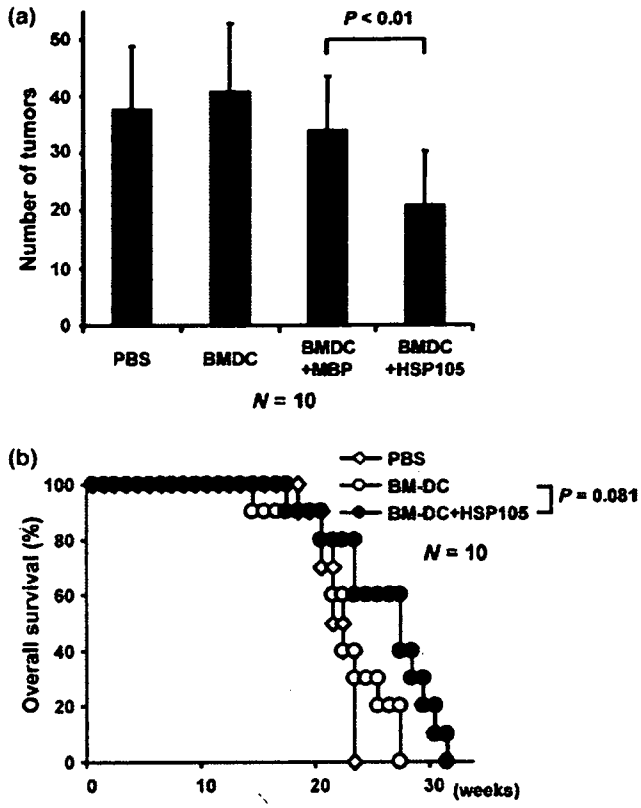

Fig. 2. Vaccination with heat shock protein (HSP) 105-pulsed bone marrow-derived dendritic cells (BM-DC) decreased the number of polyps in the small intestine of the $Apc^{Min/+}$ mice. (a) The $Apc^{Min/+}$ mice were inoculated intraperitoneally with HSP105-pulsed BM-DC (5×10^5), BM-DC alone, or myelin basic protein-pulsed BM-DC or phosphate-buffered saline (PBS) at 6, 8, and 10 weeks of age. At 12 weeks of age, the small intestines of the $Apc^{Min/+}$ mice were excised, stained with methylene blue, and the number of tumors was counted by the naked eye. Each group consisted of 10 $Apc^{Min/+}$ mice. The statistical significance of the differences in results was determined using an unpaired *t*-test. (b) The survival rate of $Apc^{Min/+}$ mice immunized with HSP105-pulsed BM-DC, BM-DC alone, or PBS as a control. The immunization protocol was the same as that of (a). The overall survival rate was calculated using the Kaplan–Meier method, and statistical significance was evaluated using Wilcoxon's test.

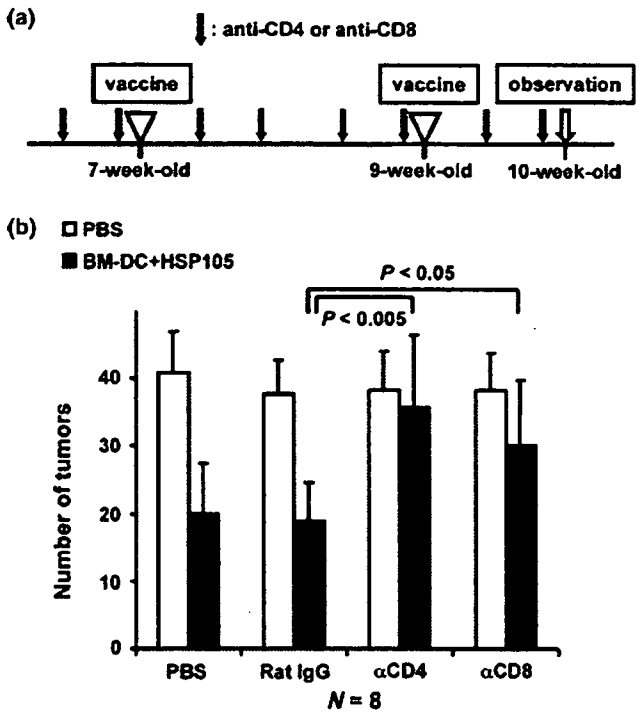

Fig. 3. Both $CD4^+$ and $CD8^+$ T cells are involved in the antitumor immunity elicited by the heat shock protein (HSP) 105-pulsed dendritic cell vaccine. (a) The protocol for the vaccination and the depletion of T cell subsets. (b) The number of polyps in the small intestine of $Apc^{Min/+}$ mice with various treatments. The number of tumors was counted as described in the legend for Fig. 2. Each group consisted of eight $Apc^{Min/+}$ mice. The statistical significance of the difference between the results was determined using the unpaired *t*-test.

the specific objective of the present study was to find out whether HSP105-pulsed DC-based immunotherapy can be used as a potent new strategy for the prevention of spontaneously arising tumors in FAP patients.

The ELISPOT assay shown in Figure 4a shows that both $CD4^+$ and $CD8^+$ HSP105-reactive T cells were primed in the mice immunized with HSP105-pulsed BM-DC. In this assay, we cannot completely rule out the possibility that responses were directed against contaminated bacteria-derived molecules in the HSP105 recombinant protein preparation. However, we consider this unlikely because practically no response was observed against BM-DC loaded with recombinant MBP protein, which was prepared from bacterial lysate in the same way as the preparation of recombinant HSP105. These recombinant proteins were purified extensively as described in a previous paper,[14] and contamination of lipopolysaccharide (LPS) or other DC-stimulants was ruled out.

Previous studies have reported that HSP105 is overexpressed specifically in a variety of human cancers and mouse tumor cells.[13,14] The present study demonstrated that HSP105 was also strongly expressed in the adenomatous polyps of $Apc^{Min/+}$ mice. In human tissue, the overexpression of HSP105 is a late event in the adenoma–carcinoma sequence, because immunohistochemical analysis revealed that HSP105 is strongly expressed in adenocarcinoma but not in adenoma.[13] Although the $Apc^{Min/+}$ mouse model has provided useful information about the pathogenesis of colorectal cancer, it is limited because it does not completely mimic the disease in humans. In humans, patients with FAP develop hundreds to thousands of adenomatous polyps, predominantly in the distal colon, and have a high risk of malignancies before the age of 40 years.[23] In contrast, $Apc^{Min/+}$ mice develop dozens to hundreds of adenomas and have a shortened life span. However, these adenomas are located mainly in the small intestine and they generally do not become malignant.[10] Furthermore, mice carrying different *Apc* mutations have been established. Tumors arising in these mice are histologically similar, but vary with respect to age of onset, number of tumors, and location.[24] Given this variation, the pattern of HSP105 expression in intestinal tumors may be different between human and $Apc^{Min/+}$ mice. Regardless of these differences, the $Apc^{Min/+}$ mice provide an appropriate model for analysis of the efficacy of the HSP105-pulsed BM-DC vaccine for inhibition of the development of human colorectal cancer, because the loss of *APC* function is the initiating event in not only FAP but also in the vast majority of sporadic colon cancers.

Recent findings regarding the cellular and molecular pathogenesis of colorectal cancer have led to the development of new targeted therapeutic options. Overexpression of COX-2 is one of the most significant observations in this respect.[25] The use of COX-2 inhibitor suppresses the development of colon cancer in

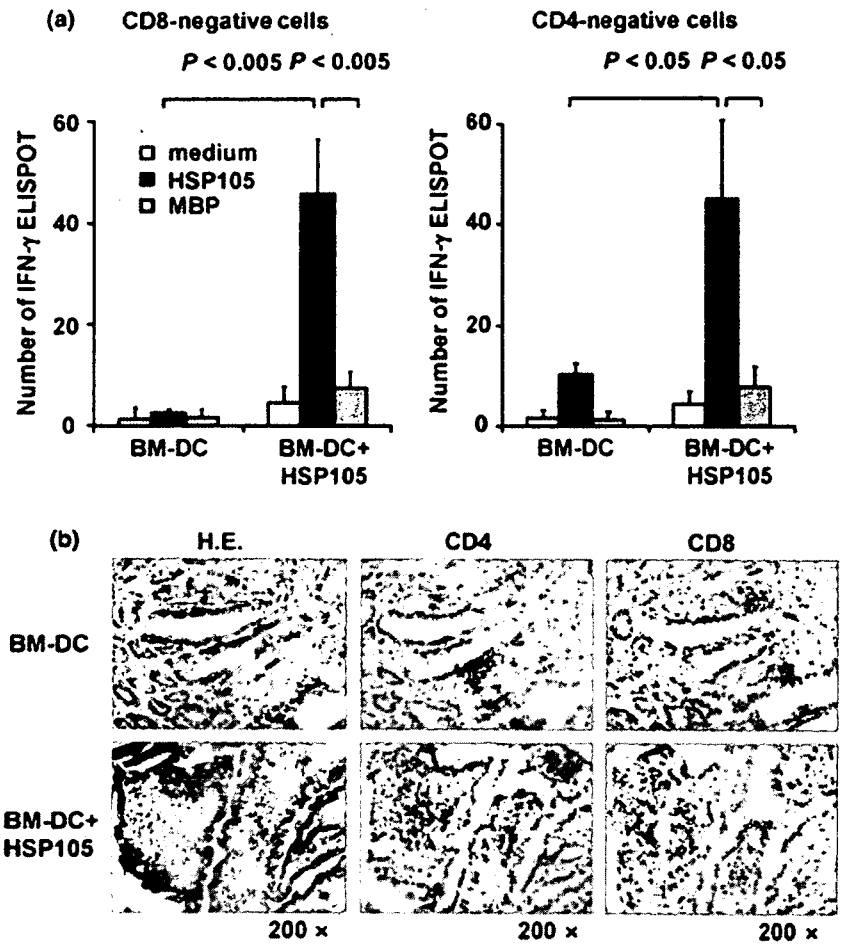

Fig. 4. Induction of heat shock protein (HSP) 105-specific T cells via immunization with HSP105-pulsed bone marrow-derived dendritic cells (BM-DC). (a) The $Apc^{Min/+}$ mice were inoculated with HSP105-pulsed BM-DC or BM-DC at 6 and 8 weeks of age. The spleen cells were harvested from 10-week-old $Apc^{Min/+}$ mice and depleted with either $CD4^+$ or $CD8^+$ cells using magnetic cell-sorting system. $CD4^-$ cells were used as a source of $CD8^+$ T cells and antigen-presenting cells, and $CD8^-$ cells were used as a source of $CD4^+$ T cells and antigen-presenting cells. Thereafter interferon-γ enzyme-linked immunospot (ELISPOT) assays were carried out. Briefly, $CD4^-$ or $CD8^-$ T cells (5×10^5) in each well were cultured together with 2 μg/mL HSP105, myelin basic protein, or medium alone for 24 h. The statistical significance of the difference in results was determined using the unpaired *t*-test. The spleens of three mice from each group were pooled. This experiment was carried out three times, with similar results. (b) The $Apc^{Min/+}$ mice were inoculated with HSP105-pulsed BM-DC or BM-DC at 6 and 8 weeks of age. The small intestines were excised from 10-week-old $Apc^{Min/+}$ mice and then were analyzed after immunohistochemical staining with anti-CD4 monoclonal antibody or anti-CD8 monoclonal antibody (magnification ×200).

sporadic cases[26] and FAP;[27] however, recent clinical trials suggest that the use of high doses of COX-2 inhibitor may have dangerous side-effects, such as increased risk of cardiovascular disease.[28] In the present study, no apparent autoimmunity was observed in the $Apc^{Min/+}$ mice immunized with HSP105-pulsed BM-DC, an observation similar to our previous findings.[14,22] In some human clinical trials of DC-based cancer immunotherapy, even in patients with advanced stages of cancer, no major toxicity nor severe side-effects were observed.[29–31] These results strongly suggest that DC-based immunotherapy is safe and feasible.

DC vaccination is now considered to be one of the most promising strategies for cancer immunotherapy.[32,33] DC are the most potent antigen-presenting cells and can present tumor antigens to stimulate a tumor-specific T-cell response. However, this does not occur in most types of cancer and in animal models of spontaneously arising tumors.[34] In the present study, immunization with HSP105-pulsed BM-DC vaccine significantly reduced the number of small-intestinal polyps in the $Apc^{Min/+}$ mice; however, the duration of survival was not prolonged as had been expected because the adenomas in $Apc^{Min/+}$ mice generally did not become malignant. Thereby, the protocol of DC-based vaccination used in the present study was not sufficient to completely prevent the occurrence of the tumors *in vivo*, and we are trying to establish a more effective immunization protocol. New strategies are now being developed to improve the clinical efficacy of DC-based vaccines, for example, the use of overexpression of Akt1 in BM-DC, suppressor of cytokine signaling 1-silenced BM-DC, and CD40-inducible DC.[35–37] The use of transfected DC in a protocol such as that used in the present study has the potential to induce a more effective antitumor response. Furthermore, it is necessary to investigate whether combinations of immunotherapy and other therapies, such as combinations of DC vaccines and chemotherapy or low-dose COX-2 inhibitors, induce a more effective antitumor response in comparison to individual therapy alone, thereby developing more effective strategies for treating colorectal cancer. Recent findings have shown the curative potential of combinations of irradiation,[38] chemotherapy,[39] and subsequent adoptive T-cell immunotherapy against established solid tumors.[40]

The abrogation of the antitumor effect of the HSP105-pulsed BM-DC vaccine, after the depletion of $CD4^+$ cells or $CD8^+$ cells via the administration of mAb, indicates that both $CD4^+$ and $CD8^+$ T cells play a critical role in the antitumor effect of HSP105-pulsed BM-DC. The report that antigen-specific $CD4^+$ T helper cells are required for the activation of $CD8^+$ effector T cells, their secondary expansion, and memory induction,[41] is consistent with the findings that $CD4^+$ T cells played an important role in tumor rejection in the present study. Peptides derived from HSP105 incorporated into BM-DC might be presented in the context of MHC class II on the surface of BM-DC to activate $CD4^+$ T cells. Subsequently, $CD4^+$ T cells produce interferon-γ and interleukin-2 to activate HSP105-specific $CD8^+$ effector T cells and facilitate the development of HSP105-specific $CD8^+$ memory T cells. Furthermore, the ELISPOT assay showed that HSP105-specific $CD8^+$ T cells were also activated by HSP105-pulsed antigen-presenting cells. These results indicate

doi: 10.1111/j.1349-7006.2007.00612.x

that HSP105-pulsed BM-DC can demonstrate peptides derived from exogenously added HSP105 not only in the context of MHC class II molecules to activate CD4+ T cells but also in the context of MHC class I molecules via the mechanism of cross-presentation to activate CD8+ T cells. Whole-protein-pulsed DC vaccines seem to be superior to peptide-pulsed DC because they can activate both CD4+ and CD8+ T cells, and it does not require a knowledge of the human leukocyte antigen (HLA) type of the cancer patients.

In conclusion, the results of the present study indicate that HSP105-pulsed BM-DC may provide a potential vaccine to combat human colorectal cancer. It is possible that immunization with HSP105-pulsed BM-DC vaccines could be useful in patients with colorectal cancer to prevent tumor recurrence after surgical resection. Although there was a noteworthy effect of this type of vaccine on the host immune response to tumors expressing HSP105, further investigation to improve the clinical efficacy of HSP105-pulsed BM-DC vaccines is called for.

Acknowledgments

This work was supported in part by Grants-in-Aid (no. 12213111 for Y. Nishimura, no. 14770142 for T. Nakatsura, and no. 14770142 for S. Senju) from the Ministry of Education, Science, Technology, Sports, and Culture, Japan, and The Sagawa Foundation for Promotion of Cancer Research and Meiji Institute of Health Science.

References

1 Weitz J, Koch M, Debus J, Hohler T, Galle PR, Büchler MW. Colorectal cancer. *Lancet* 2005; 365: 153–65.
2 Tournigand C, André T, Achille E *et al.* FOLFIRI followed by FOLFOX6 or the reverse sequence in advanced colorectal cancer: a randomized GERCOR study. *J Clin Oncol* 2004; 22: 229–37.
3 Rao CV, Cooma I, Rosa Rodriguez JG, Simi B, El-Bayoumy K, Reddy BS. Chemoprevention of familial adenomatous polyposis development in the *Apc*^{Min} mouse model by 1,4-phenylene *bis*(methylene)selenocyanate. *Carcinogenesis* 2000; 21: 617–21.
4 Kinzler KW, Vogelstein B. Cancer-susceptibility genes: gatekeepers and caretakers. *Nature* 1997; 386: 761–3.
5 Fearon ER, Vogelstein B. A genetic model for colorectal tumorigenesis. *Cell* 1990; 61: 759–67.
6 Kikuchi A. Modulation of Wnt signaling by Axin and Axil. *Cytokine Growth Factor Rev* 1999; 10: 255–65.
7 Sancho E, Batlle E, Clevers H. Signaling pathways in intestinal development and cancer. *Annu Rev Cell Dev Biol* 2004; 20: 695–723.
8 Miyoshi Y, Ando H, Nagase H *et al.* Germ-line mutations of the *APC* gene in 53 familial adenomatous polyposis patients. *Proc Natl Acad Sci USA* 1992; 89: 4452–6.
9 Su LK, Kinzler KW, Vogelstein B *et al.* Multiple intestinal neoplasia caused by a mutation in the murine homolog of the *APC* gene. *Science* 1992; 256: 668–70.
10 Moser AR, Pitot HC, Dove WF. A dominant mutation that predisposes to multiple intestinal neoplasia in the mouse. *Science* 1990; 247: 322–4.
11 Feder ME, Hofmann GE. Heat-shock proteins, molecular chaperones, and the stress response: evolutionary and ecological physiology. *Annu Rev Physiol* 1999; 61: 243–82.
12 Nakatsura T, Senju S, Yamada K, Jotsuka T, Ogawa M, Nishimura Y. Gene cloning of immunogenic antigens overexpressed in pancreatic cancer. *Biochem Biophys Res Commun* 2001; 281: 936–44.
13 Kai M, Nakatsura T, Egami H, Senju S, Nishimura Y, Ogawa M. Heat shock protein 105 is overexpressed in a variety of human tumors. *Oncol Rep* 2003; 10: 1777–82.
14 Yokomine K, Nakatsura T, Minohara M *et al.* Immunization with heat shock protein 105-pulsed dendritic cells leads to tumor rejection in mice. *Biochem Biophys Res Commun* 2006; 343: 269–78.
15 Miyazaki M, Nakatsura T, Yokomine K *et al.* DNA vaccination of HSP105 leads to tumor rejection of colorectal cancer and melanoma in mice through activation of both CD4+ T cells and CD8+ T cells. *Cancer Sci* 2005; 96: 695–705.
16 Hosaka S, Nakatsura T, Tsukamoto H, Hatayama T, Baba H, Nishimura Y. Synthetic small interfering RNA targeting heat shock protein 105 induces apoptosis of various cancer cells both *in vitro* and *in vivo*. *Cancer Sci* 2006; 97: 623–32.
17 Srivastava P. Interaction of heat shock proteins with peptides and antigen presenting cells: chaperoning of the innate and adaptive immune responses. *Annu Rev Immunol* 2002; 20: 395–425.
18 Manjili MH, Wang XY, Chen X *et al.* HSP110-HER2/neu chaperone complex vaccine induces protective immunity against spontaneous mammary tumors in HER-2/neu transgenic mice. *J Immunol* 2003; 171: 4054–61.
19 Wang XY, Chen X, Manjili MH, Repasky E, Henderson R, Subjeck JR. Targeted immunotherapy using reconstituted chaperone complexes of heat shock protein 110 and melanoma-associated antigen gp100. *Cancer Res* 2003; 63: 2553–60.
20 Dietrich WF, Lander ES, Smith JS *et al.* Genetic identification of *Mom*-1, a major modifier locus affecting *Min*-induced intestinal neoplasia in the mouse. *Cell* 1993; 75: 631–9.
21 Yamagishi N, Nishihori H, Ishihara K, Ohtsuka K, Hatayama T. Modulation of the chaperone activities of Hsc70/Hsp40 by Hsp105α and Hsp105β. *Biochem Biophys Res Commun* 2000; 272: 850–5.
22 Nakatsura T, Komori H, Kubo T *et al.* Mouse homologue of a novel human oncofetal antigen, glypican-3, evokes T-cell-mediated tumor rejection without autoimmune reaction in mice. *Clin Cancer Res* 2004; 10: 8630–40.
23 Fearnhead NS, Wilding JL, Bodmer WF. Genetics of colorectal cancer: hereditary aspects and overview of colorectal tumorigenesis. *Br Med Bull* 2002; 64: 27–43.
24 Boivin GP, Washington K, Yang K *et al.* Pathology of mouse models of intestinal cancer: consensus report and recommendations. *Gastroenterology* 2003; 124: 762–77.
25 Oshima M, Dinchuk JE, Kargman SL *et al.* Suppression of intestinal polyposis in *Apc* Δ716 knockout mice by inhibition of cyclooxygenase 2 (COX-2). *Cell* 1996; 87: 803–9.
26 Reddy BS, Hirose Y, Lubet R *et al.* Chemoprevention of colon cancer by specific cyclooxygenase-2 inhibitor, celecoxib, administered during different stages of carcinogenesis. *Cancer Res* 2000; 60: 293–7.
27 Steinbach G, Lynch PM, Philips RKS *et al.* The effect of celecoxib, a cyclooxygenase-2 inhibitor, in familial adenomatous polyposis. *N Engl J Med* 2000; 342: 1946–52.
28 Solomon SD, McMurray JJV, Pfeffer MA *et al.* Cardiovascular risk associated with celecoxib in a clinical trial for colorectal adenoma prevention. *N Engl J Med* 2005; 352: 1071–80.
29 Nestle FO, Alijagic S, Gilliet M *et al.* Vaccination of melanoma patients with peptide- or tumor lysate-pulsed dendritic cells. *Nat Med* 1998; 4: 328–32.
30 Stift A, Friedl J, Dubsky P *et al.* Dendritic cell-based vaccination in solid cancer. *J Clin Oncol* 2003; 21: 135–42.
31 Yu JS, Liu G, Ying H, Yong WH, Black KL, Wheeler CJ. Vaccination with tumor lysate-pulsed dendritic cells elicits antigen-specific, cytotoxic T-cells in patients with malignant glioma. *Cancer Res* 2004; 64: 4973–9.
32 Timmerman JM, Levy R. Dendritic cell vaccines for cancer immunotherapy. *Annu Rev Med* 1999; 50: 507–29.
33 Fong L, Engleman EG. Dendritic cells in cancer immunotherapy. *Annu Rev Immunol* 2000; 18: 245–73.
34 Gabrilovich D. Mechanisms and functional significance of tumour-induced dendritic-cell defects. *Nature Rev Immunol* 2004; 4: 941–52.
35 Park D, Lapteva N, Seethammagari M, Slawin KM, Spencer D. An essential role for Akt1 in dendritic cell function and tumor immunotherapy. *Nat Biotechnol* 2006; 24: 1581–90.
36 Evel-Kabler K, Song XT, Aldrich M, Huang XF, Chen SY. SOCS1 restricts dendritic cells' ability to break self tolerance and induce antitumor immunity by regulating IL-12 production and signaling. *J Clin Invest* 2006; 116: 90–100.
37 Hanks BA, Jiang J, Singh RAK *et al.* Re-engineered CD40 receptor enables potent pharmacological activation of dendritic-cell cancer vaccines *in vivo*. *Nat Med* 2005; 11: 130–7.
38 Reits EA, Hodge JW, Herberts CA *et al.* Radiation modulates the peptide repertoire, enhances MHC class I expression, and induces successful antitumor immunotherapy. *J Exp Med* 2006; 203: 1259–71.
39 Casares N, Pequignot MO, Tesniere A *et al.* Caspase-dependent immnogenicity of doxorubicin-induced tumor cell death. *J Exp Med* 2005; 202: 1691–701.
40 Zhang B, Bowerman NA, Salama JK *et al.* Induced sensitization of tumor stroma leads to eradication of established cancer by T cells. *J Exp Med* 2007; 204: 49–55.
41 Janssen EE, Lemmens EE, Wolfe T, Christen U, von Herrath MG, Schoenberger SP. CD4+ T cells are required for secondary expansion and memory in CD8+ T lymphocytes. *Nature* 2003; 421: 852–6.

Involvement of Regulatory T Cells in the Experimental Autoimmune Encephalomyelitis-Preventive Effect of Dendritic Cells Expressing Myelin Oligodendrocyte Glycoprotein plus TRAIL[1]

Shinya Hirata, Hidetake Matsuyoshi, Daiki Fukuma, Akari Kurisaki, Yasushi Uemura, Yasuharu Nishimura,[2] and Satoru Senju[2,3]

We previously reported the protection from myelin oligodendrocyte glycoprotein (MOG)-induced experimental autoimmune encephalomyelitis (EAE) by the adoptive transfer of genetically modified embryonic stem cell-derived dendritic cells (ES-DC) presenting MOG peptide in the context of MHC class II molecules and simultaneously expressing TRAIL (ES-DC-TRAIL/MOG). In the present study, we found the severity of EAE induced by another myelin autoantigen, myelin basic protein, was also decreased after treatment with ES-DC-TRAIL/MOG. This preventive effect diminished, if the function of $CD4^+CD25^+$ regulatory T cells (Treg) was abrogated by the injection of anti-CD25 mAb into mice before treatment with ES-DC-TRAIL/MOG. The adoptive transfer of $CD4^+CD25^+$ T cells from ES-DC-TRAIL/MOG-treated mice protected the recipient mice from MOG- or myelin basic protein-induced EAE. The number of $Foxp3^+$ cells increased in the spinal cords of mice treated with ES-DC-TRAIL/MOG. In vitro experiments showed that TRAIL expressed in genetically modified ES-DC and also in LPS-stimulated splenic macrophages had a capacity to augment the proliferation of $CD4^+CD25^+$ T cells. These results suggest that the prevention of EAE by treatment with ES-DC-TRAIL/MOG is mediated, at least in part, by MOG-reactive $CD4^+CD25^+$ Treg propagated by ES-DC-TRAIL/MOG. For the treatment of organ-specific autoimmune diseases, induction of Treg reactive to the organ-specific autoantigens by the transfer of DC-presenting Ags and simultaneously overexpressing TRAIL therefore appears to be a promising strategy. *The Journal of Immunology,* **2007, 178: 918–925.**

For the treatment of subjects with autoimmune and allergic diseases, it is desirable to down-modulate the immune response in an Ag-specific manner while not causing systemic immune suppression. To achieve this goal, genetically modified dendritic cells (DC)[4] presenting target Ags and simultaneously expressing immunoinhibitory molecules would be an attractive strategy (1).

TRAIL, a member of the TNF superfamily, is expressed in a variety of cell types, including lymphocytes, NK cells, NKT cells, and virus-infected APCs (2–5). The abrogation of functional TRAIL by gene targeting or the in vivo administration of soluble death receptor 5, one of receptors for TRAIL, results in the acceleration of autoimmune diseases in mouse models, for example collagen-induced arthritis, autoimmune diabetes, and experimental autoimmune encephalomyelitis (EAE) (6–9). It is thus evident that TRAIL plays a critical role in the regulation of the immune response or the maintenance of immunological self-tolerance to prevent autoimmunity. However, the precise mechanism for this has not yet been clarified regarding how TRAIL exerts such an effect.

We recently reported the protection from myelin oligodendrocyte glycoprotein (MOG)-induced EAE with genetically modified DC expressing MOG peptide along with TRAIL or programmed death-1 ligand (PD-L1) (1). For the genetic modification of DC, we used a method to generate DC from mouse embryonic stem cells in vitro (ES-DC) (10–13). For the efficient presentation of MOG peptide in the context of MHC class II molecules, we used an expression vector in which cDNA encoding for human MHC class II-associated invariant chain was mutated to contain antigenic peptide in the class II-associated invariant chain peptide region (14, 15). An epitope inserted into this vector is efficiently presented in the context of coexpressed MHC class II molecules. Based on these technologies, we generated transfectant ES-DC presenting MOG peptide and simultaneously expressing TRAIL or PD-L1, ES-DC-TRAIL/MOG, and ES-DC-PDL1/MOG, respectively.

The treatment of mice with either of the double-transfectant ES-DC significantly reduced the severity of MOG-induced EAE. In contrast, treatment with ES-DC expressing MOG alone, irrelevant Ag (OVA) plus TRAIL, or OVA plus PD-L1, or coinjection with ES-DC expressing MOG plus ES-DC expressing TRAIL or PD-L1, had no effect on the disease course. The immune response to irrelevant exogenous Ag (keyhole limpet hemocyanin) was not

Department of Immunogenetics, Graduate School of Medical Sciences, Kumamoto University, Kumamoto, Japan

Received for publication March 9, 2006. Accepted for publication October 31, 2006.

The costs of publication of this article were defrayed in part by the payment of page charges. This article must therefore be hereby marked *advertisement* in accordance with 18 U.S.C. Section 1734 solely to indicate this fact.

[1] This work was supported in part by Grants-in-Aid 12213111, 14370115, 14570421, 14657082, and the Program of Founding Research Centers for Emerging and Re-emerging Infectious Disease from the Ministry of Education, Science, Technology, Sports, and Culture, Japan, and a Research Grant for Intractable Diseases from the Ministry of Health, Labour and Welfare, Japan, and grants from the Uehara Memorial Foundation, and by funding from the Meiji Institute of Health Science.

[2] Y.N. and S.S. contributed equally to this study.

[3] Address correspondence and reprint requests to Dr. Satoru Senju, Department of Immunogenetics, Graduate School of Medical Sciences, Kumamoto University, Honjo 1-1-1, Kumamoto 860-8556, Japan. E-mail address: senjusat@gpo.kumamoto-u.ac.jp

[4] Abbreviations used in this paper: DC, dendritic cell; EAE, experimental autoimmune encephalomyelitis; MOG, myelin oligodendrocyte glycoprotein; ES, embryonic stem cell; PD-L1, programmed death-1 ligand; MBP, myelin basic protein; Treg, regulatory T cell; Tr1, T regulatory type 1.

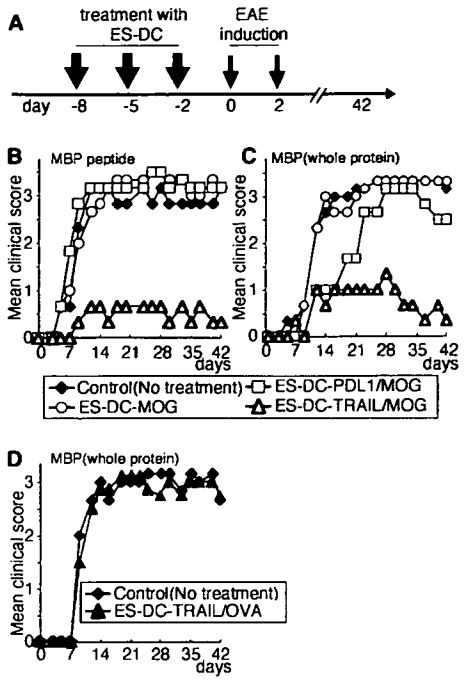

FIGURE 1. Prevention of MBP-induced EAE by treating the mice with ES-DC-TRAIL/MOG. *A*, The schedule for the pretreatment and induction of EAE is shown. CBF_1 mice (three to four mice per group) were i.p. injected with ES-DC (1×10^6 cells/mouse/injection) on days -8, -5, and -2. EAE was induced by the immunization of MBP peptide or whole protein on day 0, and the injection of *B. pertussis* toxin on days 0 and 2. *B–D*, The disease severity of mice immunized with MBP peptide (*B*) or whole protein (*C* and *D*) is shown. The data of all experiments are summarized in Table I.

impaired by treatment with any of the genetically modified ES-DC. These results suggest the possibility of treating autoimmune diseases without affecting immunity to exogenous Ags using genetically engineered DC presenting target autoantigen and simultaneously expressing TRAIL or PD-L1. In that study, we observed an increase in apoptosis of $CD4^+$ T cells in the spleens of mice treated with ES-DC-TRAIL/MOG, suggesting that protection from EAE by ES-DC-TRAIL/MOG is mediated by induction of apoptosis of MOG-reactive pathogenic $CD4^+$ T cells. In the present study, we found that the severity of not only MOG- but also myelin basic protein (MBP)-induced EAE was reduced by treatment with ES-DC-TRAIL/MOG. Regarding the mechanism underlying this disease-preventive effect, we obtained several lines of evidence supporting that MOG-reactive $CD4^+CD25^+$ regulatory T cells (Treg) were activated or propagated by the transfer of ES-DC-TRAIL/MOG and that the prevention of EAE by treatment with ES-DC-TRAIL/MOG was mediated, at least in part, by Treg.

Materials and Methods

Mice and cells

CBA and C57BL/6 mice obtained from Clea Animal or Charles River Laboratories were kept under specific pathogen-free conditions. Male CBA and female C57BL/6 mice were mated to generate F_1 (CBF_1) mice and all in vivo experiments were done using CBF_1 mice, syngeneic to TT2 ES cells. The mouse experiments were approved by the Animal Research Committee of Kumamoto University.

The mouse ES cell line, TT2, derived from CBF_1 blastocysts, and OP9 were maintained as previously described (10). The induction of differentiation of ES cells into ES-DC and generation of transfectant ES-DC-TRAIL, ES-DC-PDL1, ES-DC-MOG, ES-DC-TRAIL/MOG, ES-DC-PDL1/MOG, and ES-DC-TRAIL/OVA was done as described previously (1).

Protein, cytokines, and Abs

The mouse MOG p35–55 (MEVGWYRSPFSRVVHLYRNGK) and mouse MBP p35-47 (TGILDSIGRFFSG) were synthesized using the F-moc method on an automatic peptide synthesizer (PSSM8; Shimadzu) and purified using HPLC. Recombinant mouse GM-CSF (PeproTech) was purchased. Rat anti-mouse CD25 mAb was produced by culturing the PC61.5.3 cell line in the CELLINE system (BD Biosciences) and was purified by the MAbTrap kit (Amersham Biosciences). Abs and reagents used for staining were PE-conjugated anti-mouse CD25 (clone 3C7, rat IgG2b; BD Pharmingen) and FITC-conjugated anti-mouse CD4 (clone GK1.5, rat IgG2b; BD Pharmingen).

Induction of EAE and treatment with ES-DC

For the induction of EAE, 6- to 8-wk-old female CBF_1 mice were immunized by performing a s.c. injection at the base of tail with a 0.2-ml IFA/PBS solution containing 600 μg of MOG p35–55 peptide, MBP p35–47 peptide, or whole bovine MBP (Sigma-Aldrich), and 400 μg of *Mycobacterium tuberculosis* H37Ra (Difco Laboratories) on day 0. In addition, 500 ng of purified *Bordetella pertussis* toxin (Calbiochem) was injected i.p. on days 0 and 2 (1). For the prevention of EAE, mice were injected i.p. with ES-DC (1×10^6 cells/mouse/injection) on days -8, -5, and -2 (preimmunization treatment), or on days 14, 17, and 21 (postonset treatment). In some experiments, $CD25^+$ T cells were depleted by i.p. injections of anti-mouse CD25 mAb (clone PC61.5.3) as described (16). In brief, the mAb (400 μg/mouse) was administrated on days -28, -24, -21, and -14. Depletion was verified by staining PBMC and then analyzing them on a flow cytometer (FACScan; BD Biosciences). The mice were observed over a period of 42 or 56 days (postonset treatment) for clinical signs and scores were assigned based on the following scale: 0, normal; 1, weakness of the tail and/or paralysis of the distal half of the tail; 2, loss of tail tonicity and abnormal gait; 3, weakly partial hind-limb paralysis; 3.5, strongly partial

Table I. *Suppression of MBP-induced EAE induction in CBF_1 mice treated with ES-DC expressing MOG plus TRAIL*[a]

Treatment (ES-DC) of Mice	EAE Induced with	Disease Incidence	Day of Onset	Mean Peak Clinical Score
No treatment (control)	MBP pep	12/12	6.4 ± 1.3	3.1 ± 0.1
TRAIL/MOG	MBP pep	2/6	8.0 ± 1.0	0.7 ± 0.9
PD-L1/MOG	MBP pep	6/6	8.0 ± 2.7	3.4 ± 0.1
MOG	MBP pep	3/3	6.3 ± 1.8	3.5 ± 0.0
No treatment (control)	MBP whole	15/15	9.4 ± 1.5	3.1 ± 0.2
TRAIL/MOG	MBP whole	5/9	15.2 ± 4.6	1.0 ± 0.9
PD-L1/MOG	MBP whole	6/6	13.5 ± 3.3	3.1 ± 0.1
MOG	MBP whole	6/6	11.7 ± 0.6	3.2 ± 0.2
TRAIL/OVA	MBP whole	4/4	9.8 ± 1.1	3.3 ± 0.3
CD25 depl.[b] plus no treatment	MBP whole	6/6	10.1 ± 1.2	3.8 ± 0.5
CD25 depl.[b] plus TRAIL/MOG	MBP whole	8/8	10.0 ± 1.5	4.3 ± 1.0

[a] The data are combined from a total of nine separate experiments including those shown in Figs. 1 and 4.
[b] In these mice, $CD25^+$ cells were depleted by the treatment with anti-CD25 mAb and subsequently mice were transferred with ES-DC or left untreated. The values of onset day and mean peak clinical score are rounded off to the first decimal place.